A robust and efficient augmented free-water flash method for CO2-water-hydrocarbon mixtures

Heringer, Juan; Wapperom, Michiel; Secuianu, Catinca; Voskov, Denis; Nichita, Dan Vladimir

DOI
10.1016/j.fluid.2025.114378

Publication date
2025

Document Version
Final published version

Published in
Fluid Phase Equilibria

Citation (APA)
Heringer, J., Wapperom, M., Secuianu, C., Voskov, D., & Nichita, D. V. (2025). A robust and efficient augmented free-water flash method for CO2-water-hydrocarbon mixtures. *Fluid Phase Equilibria*, *594*, Article 114378. https://doi.org/10.1016/j.fluid.2025.114378

Fluid Phase Equilibria 594 (2025) 114378

Contents lists available at ScienceDirect

Fluid Phase Equilibria

journal homepage: www.journals.elsevier.com/fluid-phase-equilibria

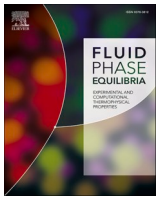

A robust and efficient augmented free-water flash method for CO_2-water-hydrocarbon mixtures

Juan Heringer [a], Michiel Wapperom [b], Catinca Secuianu [c], Denis Voskov [b,d], Dan Vladimir Nichita [a,*]

[a] CNRS UMR 5150, Laboratoire des Fluides Complexes et leurs Réservoirs, Université de Pau et des Pays de l'Adour, Pau, France
[b] Department of Geoscience and Engineering, TU Delft, The Netherlands
[c] Department of Inorganic Chemistry, Physical Chemistry and Electrochemistry, Faculty of Chemical Engineering and Biotechnologies, National University of Science and Technology "Politehnica" of Bucharest, Romania
[d] Department of Energy Science & Engineering, Stanford University, Stanford, CA, USA

ARTICLE INFO

Keywords:
Water-CO_2-hydrocarbon mixtures
Augmented free-water flash
Convergence
Efficiency
Robustness
Newton method

ABSTRACT

Three-phase equilibrium calculations for water-CO_2-hydrocarbon mixtures are required in the compositional simulation of various applications in CO_2 storage, geothermal systems, and enhanced oil recovery. The very low solubility of hydrocarbon components in water leads to a special mathematical structure of the problem. Several techniques were suggested, such as the free-water flash (FWF) and the augmented free-water flash (AFWF); in the former, the aqueous phase is pure water, while in the latter only certain components, CO_2 or methane for example, are dissolved in the aqueous phase. However, only the first-order successive substitution method was used in the previous published approaches, making them unattractive for compositional simulations in which a significant number of phase equilibrium calculations are performed. In this work, a robust and efficient AFWF method is proposed, using combined successive substitutions-modified Newton iterations. The new method is general, allowing partial solubility of any selected component in the water-rich phase, depending on the specific compositions and operating conditions. A detailed description of second-order methods in a Gibbs energy minimization framework for the general AFWF is presented. In the AFWF, the dimension of the problem and the number of function evaluations (thus the computation time) are significantly reduced. Moreover, it is shown that the augmented method always has better convergence properties than its conventional multiphase flash counterpart, in both first- and second-order methods. The new AFWF method is tested for various hydrocarbon-water-CO_2 mixtures and proved to be robust and efficient, systematically outperforming the conventional approach. Unlike in previous AFWF formulations, the number of components soluble in water is not limited, leading to a controlled accuracy with respect to a full three-phase equilibrium, even at high pressures and/or large amounts of CO_2.

1. Introduction

Three-phase equilibrium calculations for water-CO_2-hydrocarbon mixtures are required in the compositional reservoir simulation, having a wide range of applications, from important energy-transitions ones as CO_2 storage in depleted reservoirs and geothermal projects (in which thermal energy is extracted from the subsurface via CO_2 as working fluid) to a variety of enhanced oil recovery processes. When water is present in a hydrocarbon mixture, depending on composition and pressure and temperature conditions, the mixture can exhibit a three-phase equilibrium, consisting of a vapor (V), hydrocarbon-rich liquid (L) and a water-rich or aqueous (W) phase, three types of two phase equilibrium (VL, VW, LW), or to be in single phase (vapor or liquid).

A significant number of phase equilibrium calculations is required in compositional reservoir simulation. The computational effort required by thermodynamic calculations generally represents an important part of the total simulation time, leading to a low computational efficiency in large-scale reservoir simulations and when an increased number of components are considered, to describe better the physical processes taking place in the reservoir. Robustness of the phase equilibrium solver is also essential, since a failure during a simulation run may lead to

* Corresponding author.
E-mail address: dnichita@univ-pau.fr (D.V. Nichita).

https://doi.org/10.1016/j.fluid.2025.114378
Received 22 December 2024; Received in revised form 6 February 2025; Accepted 11 February 2025
Available online 12 February 2025

Nomenclature

c_i	asymptotes of MRR function
f_i	fugacity of component i
G	Gibbs free energy
g	gradient
H	Hessian matrix
I	identity matrix
J	Jacobian matrix
K_i	equilibrium constant
L	hydrocarbon-rich liquid phase fraction
nc	number of components
n	mole numbers
P	pressure
R	LHS of RR equation
S	convergence matrix
T	temperature
U	ideal part of Hessian matrix
V	vapor phase fraction
W	water-rich liquid phase fraction
x_i	mole fraction of component i in liquid phase
x_w	mole fraction of water in liquid phase
y_i	mole fraction of component i in vapor phase
y_w	mole fraction of water in vapor phase
w_i	mole fraction of component i in water-rich phase
w_w	mole fraction of water in water-rich phase
z_i	feed composition

Greek letters

ε	tolerance
φ_i	fugacity coefficient of component i
ω	acentric factor
Φ	residual part of Hessian matrix

Subscripts

i, j	component index
c	critical
V	vapor phase index
L	hydrocarbon rich liquid phase index
W	aqueous phase index

Superscripts

(k)	iteration number

erroneous results or interruption of the simulation.

A variety of multiphase equilibrium calculation algorithms were proposed for mixtures containing water (Sabet and Gahrooei [1], Mortezazadeh and Rasaei [2], Nazari et al. [3], Connolly et al. [4], Imai et al. [5], Li and Li [6], Petitfrere et al. [7], Ma et al. [8], Sun et al. [9]). Algorithms for water-inclusive mixtures at pressure and enthalpy specifications were presented by Zhu and Okuno [10], Huang and Yang [11] and Huang et al. [12]. These methods are using full three-phase flash calculations, that is, with no assumptions concerning the aqueous phase, which contains all components present in the mixture.

However, the particularity of water-hydrocarbon mutual solubility can be exploited to simplify phase equilibrium algorithms. The solubility of hydrocarbon components in the aqueous phase is several orders of magnitude smaller than the solubility of water in the hydrocarbon-rich phase. Based on this observation, in the free-water assumption [13–15] the solubility of hydrocarbon components in the aqueous phase is neglected and this phase is considered pure water. Tang and Saha [13] presented the first FWF method based on a modified Rachford-Rice (MRR) equation. Iranshahr et al. [14] used an even more restricted model (neglecting also the solubility of water in the hydrocarbon-rich liquid phase) in compositional EoS based reservoir simulation. Lapene et al. [15] observed that MRR functions in Refs. [13,14] are not monotonic and they proposed a new MRR equation, which is monotonic within the feasible interval. Li and Li [16] used the latter MRR and proposed a restricted feasible domain. The advantage of the FWF is that it replaces the three-phase problem with a pseudo-two-phase problem; the MRR equation is solved for one variable, instead of solving a three-phase Rachford-Rice problem, which consists of a system of two nonlinear equations. The FWF was extended to four-phase equilibrium (Li et al. [17]) and adapted to other phase equilibrium problems having a similar mathematical structure, such as vapor-liquid-asphaltene three-phase equilibrium (Chen et al. [18,19]) and chemical and phase equilibria of mercury in natural gas (Koulocheris et al. [20]). Several implementations of the FWF in compositional simulations were presented by Cremon et al. [21] and Cremon and Gerritsen [22,23].

The FWF procedures have a very good accuracy for low to moderate pressures and for relatively small amounts of water and CO_2. Their limitation is that at high pressures, the deviations from the results obtained with a full three-phase flash are increasing and a percentage of 2–5% of CO_2 dissolved in the aqueous phase cannot be neglected any more [24]. Mole fractions of methane [25] and other light hydrocarbon components (as will be shown in the results section of this work) in the aqueous phase may also increase with pressure and the solubility of these components in water must be considered for certain phase equilibrium problems.

Early attempts to take into account the solubility of CO_2 in water using Henry's law were presented by Li and Nghiem [26] and by Enick and Klara [27]. Yan et al. [28] and Yan and Stenby [29,30] solved the three-phase VLW problem in compositional reservoir simulation of various enhanced oil recovery processes, by using different solubility scenarios, from free-water to arbitrary numbers of components in water, in an attempt to maintain a high level of simplicity in describing the three-phase equilibrium in the code. It appeared that neglecting the solubility of CO_2 in water might affect to a high extent the results of simulations. However, no details on the implementation were given in Refs. [28–30]; a description of simplified flash calculations in hydrocarbon mixtures can be found in Ref. [31].

Pang and Li proposed the so-called augmented free-water flash, in which the algorithm is considering only the solubility of one component in the aqueous phase, that is, CO_2 [24] or methane [25]. A detailed description of the simplified SSI method using a modified multiphase Rachford-Rice equation is presented and an initialization procedure for the AFWF is proposed in Refs. [24,25].

To date, the first-order SSI method was used in all papers in the open literature presenting different implementations of FWF and AFWF (only unpublished materials dealt with Newton methods for FWF [32] and AFWF [31]). In the context of compositional reservoir simulation, the potentially very slow SSI method is not suitable (except maybe at low pressures as in some thermal oil recovery methods) and faster methods such as second-order Newton iteration must be considered.

In this study, a general approach for partial solubility of selected components in the water-rich phase is developed, in which first- (SSI) and second order (Newton) methods are applied to solve two- and three-phase equilibrium problems for hydrocarbon/water/CO_2 mixtures. The algorithm is inspired by the AFWF, but instead of considering only one dissolved component in the aqueous phase, the solubility of an arbitrary number of components is considered. Moreover, the fact that we use a second order method for stability test and phase split calculation reduces considerably the computational time. The cubic two-parameter Peng-Robinson equation of state is used, but the proposed method is not

model-dependent (any thermodynamic model can be used to describe the equilibrium phases). To the best of our knowledge, second-order methods for the AFWF are presented in detail for the first time in this work.

The paper is structured as follows. First, the formalism and calculation algorithm for the general augmented free-water flash with partial solubility in the aqueous phase are presented in detail. Then, the new algorithm is tested for several CO_2-water-hydrocarbon mixtures from the literature, and results are compared with those of FWF and full three-phase flash, in term of accuracy and convergence speed. Finally, the differences between methods are discussed before concluding. Two appendices present the derivation of the Q-function from the Gibbs free energy and the input data used by the EoS model.

2. General AFWF

A general AFWF for three-phase equilibrium in water-CO_2-hydrocarbon mixtures is presented, allowing dissolution of selected components in the aqueous phase, using a combined SSI-Newton method. We note with m the number of components present in the water-rich phase and $ns = m - 1$ is the number of components soluble in water. Without losing generality, the ordering in the list of components is: $i = 1$ for water, $i = 2, m$ for components soluble in water and $i = m + 1, nc$ for components with neglected solubility in water.

2.1. Material balance equations

The component material balance equations are

$$z_i = n_{iV} + n_{iL} + n_{iw} = Vy_i + Lx_i + Ww_i; i = 1, m \tag{1a}$$

$$z_i = n_{iV} + n_{iL} = Vy_i + Lx_i; i = m + 1, nc \tag{1b}$$

and the overall material balance equation is

$$V + L + W = 1 \tag{2}$$

Component mole fractions are subjected to

$$\sum_{i=1}^{nc} y_i = \sum_{i=1}^{nc} x_i = \sum_{i=1}^{m} w_i = \sum_{i=1}^{nc} z_i = 1 \tag{3}$$

The two sets of equilibrium ratios are defined, taking for convenience the liquid phase as reference

$$K_{iV} = \frac{y_i}{x_i} = \frac{\varphi_{iL}}{\varphi_{iV}};\ i = 1, nc \tag{4a}$$

$$K_{iW} = \frac{w_i}{x_i} = \frac{\varphi_{iL}}{\varphi_{iW}};\ i = 1, m \tag{4b}$$

From Eqs. (1), (2) and (4), the mole fractions are

$$x_i = \frac{z_i}{E_i}; i = 1, m \tag{5a}$$

$$x_i = \frac{z_i}{\bar{E}_i}; i = m + 1, nc \tag{5b}$$

$$y_i = \frac{z_i K_{iV}}{E_i}; i = 1, m \tag{6a}$$

$$y_i = \frac{z_i K_{iV}}{\bar{E}_i}; i = m + 1, nc \tag{6b}$$

$$w_i = \frac{z_i K_{iW}}{E_i}; i = 1, m \tag{7}$$

where

$$E_i = 1 + V(K_{iV} - 1) + W(K_{iW} - 1); i = 1, m \tag{8a}$$

$$\bar{E}_i = 1 + V(K_{iV} - 1) - W; i = m + 1, nc \tag{8b}$$

2.2. Minimization of Gibbs free energy

The dimensionless Gibbs free energy for a three-phase VLW system is

$$G = \sum_{j=1}^{np} \sum_{i=1}^{nc} n_{ij} \ln f_{ij} = \sum_{j=1}^{np-1} \sum_{i=1}^{nc} n_{ij} \ln f_{ij} + \sum_{i=1}^{nc} n_{iw} \ln f_{iw} \tag{9}$$

If the aqueous phase contains only $m < nc$ components, G is

$$G = \sum_{i=1}^{nc} n_{iV} \ln f_{iV} + \sum_{i=1}^{nc} n_{iL} \ln f_{iL} + \sum_{i=1}^{m} n_{iW} \ln f_{iW} \tag{10}$$

The $nc+m$ independent variables are $n_{iV}; i = 1, nc$ and $n_{iW}; i = 1, m$. The vector of independent variables is $\mathbf{n} = (n_1, ..., n_{nc+m})^T = (n_{1V}...., n_{nc,V}, n_{1W}, ..., n_{mW})^T$, with $n_i = n_{iV}; i = 1, nc$ and $n_i = n_{i-nc,W}; i = nc + 1, nc + m$.

The gradient is

$$g_i = \frac{\partial G}{\partial n_{iV}} = \ln f_{iV} - \ln f_{iL} = \ln K_{iV} + \ln \varphi_{iV} - \ln \varphi_{iL}; i = 1, nc \tag{11a}$$

$$g_{i+nc} = \frac{\partial G}{\partial n_{iW}} = \ln f_{iW} - \ln f_{iL} = \ln K_{iW} + \ln \varphi_{iW} - \ln \varphi_{iL}; i = 1, m \tag{11b}$$

The stationarity conditions of G represent a nonlinear system of equations

$$\mathbf{g}(\mathbf{n}) = \mathbf{0} \tag{12}$$

2.3. Newton iterations

2.3.1. Mole numbers as independent variables

The Newton iteration equation is

$$\mathbf{H}\Delta\mathbf{n} = -\mathbf{g} \tag{13}$$

and mole numbers are updated after solving the linear system of equations, by $\mathbf{n}^{(k+1)} = \mathbf{n}^{(k)} + \Delta\mathbf{n}^{(k)}$.

The linear system Eq. (13) has a block structure and can be written as

$$\begin{pmatrix} \mathbf{H}_{VV} & \mathbf{H}_{VW} \\ \mathbf{H}_{WV} & \mathbf{H}_{WW} \end{pmatrix} \cdot \begin{pmatrix} \Delta\mathbf{n}_V \\ \Delta\mathbf{n}_W \end{pmatrix} = -\begin{pmatrix} \mathbf{g}_V \\ \mathbf{g}_W \end{pmatrix} \tag{14}$$

where $\mathbf{H}_{VV}$ is an $[nc \times nc]$ matrix, $\mathbf{H}_{VW}$ is an $[nc \times m]$ matrix, $\mathbf{H}_{WV} = \mathbf{H}_{VW}^T$ and $\mathbf{H}_{WW}$ is an $[m \times m]$ matrix. The elements of the vector $\mathbf{g}_V$ are $g_{V,i} = g_i; i = 1, nc$ and the vector $\mathbf{g}_W$ is $g_{W,i} = g_i; i = nc + 1, nc + m$. Subscripts V and W correspond to the phase index of mole numbers in the first- and second-order partial derivatives.

The Hessian matrix

$$\mathbf{H} = \mathbf{U} + \mathbf{\Phi} \tag{15}$$

has an ideal part $\mathbf{U}$, depending only on phase compositions and a non-ideal part $\mathbf{\Phi}$ containing partial derivatives of fugacity coefficients with respect to mole numbers.

The elements of the matrix $\mathbf{U}$ are

$$U_{ij} = U_{VV_{i,j}} = \frac{1}{V}\left(\frac{\delta_{ij}}{y_i} - 1\right) + \frac{1}{L}\left(\frac{\delta_{ij}}{x_i} - 1\right); i, j = 1, nc \tag{16a}$$

$$U_{i,nc+j} = U_{VW_{i,j}} = \frac{1}{L}\left(\frac{\delta_{ij}}{x_i} - 1\right); i = 1, nc; j = 1, m \tag{16b}$$

$$U_{i+nc,j} = U_{WV_{i,j}} = \frac{1}{L}\left(\frac{\delta_{ij}}{x_i} - 1\right); i = 1, m; j = 1, nc \tag{16c}$$

$$U_{i+nc,j+nc} = U_{WW_{i,j}} = \frac{1}{W}\left(\frac{\delta_{ij}}{w_i} - 1\right) + \frac{1}{L}\left(\frac{\delta_{ij}}{x_i} - 1\right); i,j = 1,m \tag{16d}$$

and the elements of the matrix $\mathbf{\Phi}$ are

$$\Phi_{ij} = \Phi_{VV_{i,j}} = \frac{\partial \ln\varphi_{iV}}{\partial n_{jV}} + \frac{\partial \ln\varphi_{iL}}{\partial n_{jL}}; i,j = 1,nc \tag{17a}$$

$$\Phi_{i,nc+j} = \Phi_{VW_{i,j}} = \frac{\partial \ln\varphi_{iL}}{\partial n_{jL}}; i = 1,nc; j = 1,m \tag{17b}$$

$$\Phi_{i+nc,j} = \Phi_{WV_{i,j}} = \frac{\partial \ln\varphi_{iL}}{\partial n_{jL}}; i = 1,m; j = 1,nc \tag{17c}$$

$$\Phi_{i+nc,j+nc} = \Phi_{WW_{i,j}} = \frac{\partial \ln\varphi_{iW}}{\partial n_{jW}} + \frac{\partial \ln\varphi_{iL}}{\partial n_{jL}}; i,j = 1,m \tag{17d}$$

The gradient norm is

$$S_g = \left(\sum_{i=1}^{nc+m} g_i\right)^{0.5} \tag{18}$$

and iterations are stopped when $S_g < \varepsilon$.

A modified Cholesky factorization [33,34] is used to restore positive definiteness of the Hessian matrix when some of its eigenvalues become negative during Newton iterations. It consists in a diagonal correction by adding some elements on the main diagonal of the Hessian and solve $(\mathbf{H} + \mathbf{E})\Delta\boldsymbol{\xi}^{(n)} = -\mathbf{g}$. A line search on the Newton direction is performed to ensure that the Gibbs free energy is decreased at each iteration level, using the procedure described in Ref. [35]. Note that trust-region methods can be alternatively used, following the implementation in Ref. [36].

2.3.2. Natural logarithms of equilibrium constants as independent variables

If the natural logarithms of the equilibrium constants are the independent variables, the Newton iteration equation is

$$\mathbf{J}\Delta\mathbf{lnK} = -\mathbf{g} \tag{19}$$

where $\mathbf{lnK} = (\ln K_1, ..., \ln K_{nc+m})^T = (\ln K_{1V}, ..., \ln K_{nc,V}, \ln K_{1W}, ..., \ln K_{mW})^T$ is the vector collecting the natural logarithms of equilibrium constants, with $\ln K_i = \ln K_{iV}; i = 1,nc$ and $\ln K_i = \ln K_{i-nc,W}; i = nc + 1, nc + m$.

The Jacobian matrix is

$$\mathbf{J} = \mathbf{H}\mathbf{U}^{-1} = \mathbf{I} + \Phi\mathbf{U}^{-1} \tag{20}$$

with elements

$$J_{ij} = \frac{\partial g_i}{\partial \ln K_j}; i,j = 1, nc + m \tag{21}$$

or

$$J_{ij} = \sum_{k=1}^{nc+m} H_{ik}U_{kj}^{-1} = \sum_{k=1}^{nc+m} \frac{\partial g_i}{\partial n_k}\frac{\partial n_k}{\partial \ln K_j}; i,j = 1, nc + m \tag{22}$$

Calculation of $\mathbf{U}^{-1}$ elements for multiphase equilibrium is tedious. The calculation procedure from Petitfrere and Nichita [37] can be readily adapted to the AFWF. However, effective calculation of $\mathbf{U}^{-1}$ can be avoided by solving $\mathbf{H}\Delta\mathbf{n} = -\mathbf{g}$ for $\Delta\mathbf{n}$, then use the relation

$$\Delta\mathbf{lnK} = \mathbf{U}\Delta\mathbf{n} \tag{23}$$

to update equilibrium constants from $\mathbf{lnK}^{(k+1)} = \mathbf{lnK}^{(k)} + \Delta\mathbf{lnK}^{(k)}$. This procedure is equivalent of solving directly Eq. (19) for $\Delta\mathbf{lnK}$ and was first proposed by Michelsen [38]. Note that in this case the Hessian and the gradient are evaluated at $\mathbf{n}^{(k)}$ calculated from equilibrium constants $\mathbf{K}^{(k)}$ via the Rachford-Rice equations.

Although not used in this work, note that Newton iterations with lnK as independent variables are suitable for including the negative flash [39–42] option.

2.4. SSI iterations

In the SSI method, the equilibrium constants are updated in an outer loop and phase mole fractions are calculated in an inner loop at constant K-values by solving the Rachford-Rice equations. If in the expression of the Jacobian matrix the partial derivatives of the fugacity coefficients with respect to mole numbers (elements of the $\mathbf{\Phi}$ matrix) are neglected, that is, $\mathbf{J} = \mathbf{I}$, the SSI iteration equation (outer loop) is

$$\Delta\mathbf{lnK} = -\mathbf{g} \tag{24}$$

which is equivalent of updating the $nc+m$ equilibrium constants from Eqs (4).

The SSI methods of Lapene et al. [15] for FWF and of Pang and Li [24,25] are particular cases of our procedure for m=1 and m=2, respectively.

The convergence rate of the SSI method is controlled by the maximum eigenvalue of the convergence matrix $\mathbf{S}$ [38], with elements

$$S_{ij} = \left(\frac{\partial \ln K_i^{(\nu+1)}}{\partial \ln K_i^{(\nu)}}\right)_{\nu\to\infty}; i,j = 1, nc + m \tag{25}$$

or

$$\mathbf{S} = \mathbf{I} - \mathbf{J} \tag{26}$$

The SSI method is linearly convergent to a local (at least) minimum of the Gibbs free energy [38]. Converge requires that $\rho_S < 1$, where the spectral radius is

$$\rho = \max_i |\lambda_i|; i = 1, nc + m \tag{27}$$

Two eigenvalues of $\mathbf{S}$ are equal unity exactly at the critical point [38], or on the convergence locus for the negative flash [39,40].

The switch to the second-order method is performed either after a predetermined small number of SSI iterations, or at a certain value of the Euclidean norm of the gradient, which can be predetermined or calculated using some switching criteria indicating that the SSI iterations became too slow.

2.5. Rachford Rice equations

The Rachford-Rice equations are solved for phase mole fractions in the inner loop of flash calculations (with lnK as independent variables) at constant K-values. Starting from the equations

$$\sum_{i=1}^{nc} (y_i - x_i) = 0 \tag{28a}$$

$$\sum_{i=1}^{m} w_i - \sum_{i=1}^{nc} x_i = 0 \tag{28b}$$

and combining Eqs. (5) to (7) and Eqs. (28), the Rachford-Rice equations for AFWF are

$$R_V(V,W) = \sum_{i=1}^{m} \frac{z_i(K_{iV} - 1)}{E_i} + \sum_{i=m+1}^{nc} \frac{z_i(K_{iV} - 1)}{\overline{E}_i} = 0 \tag{29a}$$

$$R_W(V,W) = \sum_{i=1}^{m} \frac{z_i(K_{iW} - 1)}{E_i} - \sum_{i=m+1}^{nc} \frac{z_i}{\overline{E}_i} = 0 \tag{29b}$$

The Q function for AFWF is

$$Q(V,W) = -\sum_{i=1}^{m} z_i \ln E_i - \sum_{i=m+1}^{nc} z_i \ln \overline{E}_i \tag{30}$$

and the Rachford-Rice equations are exactly the zero-gradient equations of Q with changed signs.

$$\frac{\partial Q}{\partial V} = -R_V(V,W) \tag{31a}$$

$$\frac{\partial Q}{\partial W} = -R_W(V,W) \tag{31b}$$

The Q function can be derived directly from the expression of the Gibbs free energy (as shown in Appendix A). The Q functions used by Pang and Li [24,25] and their modified Rachford-Rice equations for only one component soluble in water (CO_2 [24] or methane [25]) are particular cases of Eqs. (31) and of Eqs. (30), respectively. The function Q is convex, since the Hessian of Q is positive semi-definite [42,43] within the feasible domain (the negative flash window [41]) defined by the conditions $E_i > 0; i = 1,m$ and $\overline{E}_i > 0; i = m+1,nc$.

The bounds of a restricted feasible domain (Okuno et al. [43]), as an extension of those proposed by Pang and Li [24,25] are

$$V(1-K_{iV}) - W(1-K_{iW}) \le \min_i\{1-z_i, 1-K_{iV}z_i, 1-K_{iW}z_i\}; i = 1,m \tag{32a}$$

$$V(1-K_{iV}) + W \le \min_i\{1-z_i, 1-K_{iV}z_i\}; i = m+1,nc \tag{32b}$$

The function Q is minimized using a Newton method with line search as in Okuno et al. [44]. An inexact line search with quadratic and cubic backtracking is used.

2.6. Two-phase AFWF

The calculation procedure starts with a three-phase AFWF. If a detected infeasibility of the three-phase RR indicates the absence of the aqueous phase or if the aqueous phase vanishes during iterations (unless a negative flash is performed), a conventional VL two-phase flash of dimension nc is carried out (details on two-phase VL flash can be found in Refs. [36,45]).

If one of the hydrocarbon-rich phases vanishes, a WV (here V stands for convenience for the hydrocarbon-rich phase, which may be vapor or liquid) two-phase AFWF with only m variables described below is carried out.

In the VW case, the component material balance equations are

$$z_i = n_{iV} + n_{iw} = Vy_i + Ww_i; i = 1,m \tag{33a}$$

$$z_i = n_{iV} = Vy_i; i = m+1,nc \tag{33b}$$

and the overall material balance equation is

$$V + W = 1 \tag{34}$$

The equilibrium constants (taking water as the reference phase) are

$$K_i = \frac{y_i}{w_i} = \frac{\varphi_{iW}}{\varphi_{iV}};\ i = 1,m \tag{35}$$

The mole fractions are

$$w_i = \frac{z_i}{E_i}; i = 1,m \tag{36}$$

$$y_i = \frac{z_i K_i}{E_i}; i = 1,m \tag{37a}$$

$$y_i = \frac{z_i}{V}; i = m+1,nc \tag{37b}$$

where

$$E_i = 1 + V(K_i - 1); i = 1,m \tag{38}$$

The Rachford-Rice equation is

$$\sum_{i=1}^{m} w_i - \sum_{i=1}^{nc} x_i = \sum_{i=1}^{m} \frac{z_i(K_{iW}-1)}{E_i} - \frac{1}{V}\sum_{i=m+1}^{nc} z_i = 0 \tag{39}$$

or, using Muskat's notation [46], $c_i = 1/(1 - K_{iW}); i = 1,m$

$$\sum_{i=1}^{m} \frac{z_i}{V - c_i} - \frac{1}{V}\sum_{i=m+1}^{nc} z_i = 0 \tag{40}$$

In this case, the function Q is

$$Q(V) = -\sum_{i=1}^{m} z_i \ln E_i - \ln V \sum_{i=m+1}^{nc} z_i \tag{41}$$

However, in two-phase flash calculations, it is more convenient to solve the nonlinear Rachford-Rice equation than to minimize Q. The Rachford-Rice equation is solved using convex transformations (Nichita and Leibovici [47,48]). In this case, the change of variables is $a = V/(c_w - V); a > 0$.

The dimensionless Gibbs free energy for a VW equilibrium is

$$G = \sum_{i=1}^{nc} n_{iV} \ln f_{iV} + \sum_{i=1}^{m} n_{iW} \ln f_{iW} \tag{42}$$

and the gradient is

$$g_i = \frac{\partial G}{\partial n_{iV}} = \ln f_{iV} - \ln f_{iW} = \ln K_i + \ln \varphi_{iV} - \ln \varphi_{iW}; i = 1,m \tag{43}$$

The elements of the Hessian matrix $\mathbf{H} = \mathbf{U} + \mathbf{\Phi}$ are

$$U_{i,j} = \frac{1}{W}\left(\frac{\delta_{ij}}{w_i} - 1\right) + \frac{1}{V}\left(\frac{\delta_{ij}}{y_i} - 1\right); i,j = 1,m \tag{44}$$

and

$$\Phi_{i,j} = \frac{\partial \ln \varphi_{iW}}{\partial n_{jW}} + \frac{\partial \ln \varphi_{iV}}{\partial n_{jV}}; i,j = 1,m \tag{45}$$

2.7. Initialization

The equilibrium ratio of water component in the vapor phase is [15]

$$K_{wV} = \frac{P}{P_{cw}}\frac{T_{cw}}{T} \tag{46}$$

where P_{cw} and T_{cw} are the critical temperature and pressure of water. For the other components the K-values are calculated using the Wilson equation [49]

$$K_{iV} = \frac{P_{ci}}{P} exp\left[5.37(1+\omega_i)\left(1 - \frac{T_{ci}}{T}\right)\right]; i = 2,nc \tag{47}$$

and ω_i is the component acentric factor.

The initial guess for mole fraction of water component in vapor phase is [15]

$$y_w = \frac{P^w_{sat}}{P} \tag{48}$$

where y_w is the phase fraction of water component in vapor phase, P^w_{sat} is the vapor pressure of pure water and its values are calculated according to Antoine law.

The expression of K_{wW} is obtained by combining the definition equations of equilibrium ratios, $x_w = y_w/K_{wV}$ and $K_{wW} = w_w/x_w$, giving [25]

$$K_{wW} = \frac{K_{iW}}{y_w} w_w \tag{49}$$

The mole fraction of water component is the aqueous phase in Eq. (49) is set to $w_w = 1$ as in FWF and the eequilibrium ratios in the water-

rich phase are defined as in Refs. [24,25]

$$K_{iW} = \begin{cases} K_{wW}; & i = 1 \\ 0.5/K_{wW}; & i = 2, m \\ 0; & i = m+1, nc \end{cases} \quad (50)$$

The empirical correction of K_{wW} calculated with Eq. (49) is [24]

$$K_{wW}^{new} = -0.1K_{wW}^2 + 1.9K_{wW}; K_{wW} > 3.2 \quad (51)$$

In this work, the initialization scheme based on ideal and empirical equilibrium constants from Lapene et al. [15] and Pang and Li [24,25] presented above was used. Note that starting from poor initial guesses represents a supplementary test for the robustness of the method. An initialization strategy using sequential phase stability and flash calculations [38,50], tailored for AFWF, which takes full advantage of the particularities of hydrocarbon-water-CO_2 phase equilibrium and of the AFWF assumption (partial solubility in the aqueous phase) is being currently developed by our research team.

3. Results and discussion

In this section, the proposed method for augmented free-water flash with partial solubility in the liquid water phase, is validated in terms of efficiency and robustness using three different hydrocarbon-water mixtures. This method is compared with the results obtained from the free-water flash and the conventional multiphase flash, which will serve as the reference for the tests conducted. The tests with an increasing number of components soluble in the water phase show how close to the reference solution the new algorithm can get. Furthermore, the efficiency of the method is investigated by considering the number of iterations in phase split calculation as a parameter. Three-phase envelopes, phase fractions and mole fractions are used to verify the deviation of the results from both free-water flash and the proposed method with respect to the conventional three-phase flash algorithm. For the results using the AFWF, an integer number, **ns** will identify the number of components soluble in the aqueous phase. The enumeration follows the order given by the tables of properties of mixtures. The Peng-Robinson EoS [51,52] is used in all examples. The tolerance for flash calculations is 1e-10 and the switch criterion to pass from the SSI to Newton is 1e-2 in all examples.

3.1. Water/CO_2/North Ward Estes (NWE) oil mixture

This fluid consists in a mixture of CO_2/water/NWE-oil from Pang and Li [24]. Table B1 shows the components' properties and Table B2 presents the binary interaction parameters (BIPs).

3.1.1. Accuracy of FWF and AFWF

The phase envelope of water/CO_2/NWE-oil mixture is shown in Fig. 1 and is in good agreement with Ref. [24]. In Table 1, the results for phase fractions and mole fractions of each phase are listed for the water/CO_2/NWE-oil mixture at 400 bar and 600 K. For this case, the methods used are full three-phase flash, FWF and AFWF using one and five components dissolved in water phase. The AFWF with *ns*=1 is already close to the reference solution, while for *ns*=5 the results are even closer to the full flash results. However, for the FWF, the results are relatively distant from the full three-phase flash. In this particular case, at high pressure and temperature, the effect of solubility of components in the water phase is not negligible and may cause significant discrepancies in the calculated compositions, as confirmed by the results shown in Table 1. At a higher pressure, 470 bar, and temperature, 620 K (see Table 2), the deviation is more pronounced in AFWF with only CO_2 dissolved in the aqueous phase, and in the FWF only two phases appear.

The lower the number of components considered in the water-rich phase, the higher is the difference in composition as compared to the conventional method. In addition, this test shows that trace components

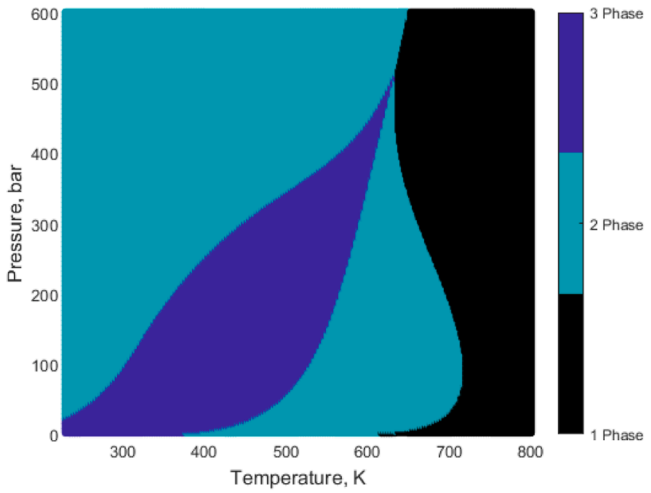

Fig. 1. Phase envelope of the water/CO_2/NWE-oil mixture.

can be handled by applying the same procedure; once a component reaches a certain minimum value, the algorithm can disregard this component in that particular phase, with negligible influence on the accuracy and reduction of the computational time. Such a strategy is possible since the proposed algorithm gives the flexibility to choose the number of components dissolved in the aqueous phase.

The phase envelopes in Fig. 2 for full three-phase flash, FWF and AFWF were constructed by performing flash calculations in the whole domain, with small pressure and temperature steps. The FWF deviates from the expected solution when the pressure and temperature are higher, more specifically in a temperature range from 550 K to 630 K and pressure interval from 300 bar to 540 bar. For the AFWF, the results show good agreement with the expected solution, with the exception to the case that considers only CO_2 dissolved in the water phase. This can be seen more clearly when looking at the detail in Fig. 3, which shows a significant difference between the results of FWF and AFWF with only CO_2 dissolved, with respect to the full three-phase flash. On the other hand, when three or more components are considered in the water-rich phase, the results are very close to those of the full flash.

Further comparison of the flash methods is done considering the phase fraction distribution with respect to temperature for a pressure of 400 bar, as presented in Fig. 4. In the AFWF, one and five components are considered. Results for FWF have a significant deviation, especially for higher temperatures, when compared to the ones obtained from AFWF, which gives basically the same result as the reference method. Another phase fraction distribution verification is done in Fig. 5, but in this case temperature is kept constant and pressure is varied. For this case, both FWF and AFWF have close values with respect to the three-phase conventional flash at lower pressures, but as pressure increases deviations become evident.

3.1.2. Convergence analysis

In this section, the convergence behavior of first- and second- order methods is analyzed for FWF, AFWF, and full three-phase flash.

The convergence rate of the SSI method is controlled by the maximum eigenvalue (absolute value) of the convergence matrix **S** in Eq. (25) [38]. The higher the spectral radius of **S**, the slower is the convergence of SSI. The elements of the matrix **S** are calculated at the solution, as well as its eigenvalues. In Table 3, the spectral radius, number of iterations and phase fractions are presented for the SSI method applied to the full flash and to the augmented method considering one and five components soluble in water. As expected, the number of iterations increases when the value of the maximum eigenvalue increases.

The spectral radius plays a significant role when pressure and

Table 1
Comparison of phase compositions obtained with the three different methods for the water/CO_2/NWE-oil mixture at 400 bar and 600 K.

Component	Full Three-Phase Flash			Three-Phase FWF			Three-Phase AFWF- 1			Three-Phase AFWF - 5		
	y_i	x_i	w_i	y_i	x_i	w_i	y_i	x_i	w_i	y_i	x_i	w_i
H_2O	0.4486	0.3197	0.9605	0.4872	0.3260	1.0000	0.4529	0.3202	0.9668	0.4486	0.3197	0.9605
CO_2	0.2944	0.2517	0.0359	0.2810	0.2378	-	0.2927	0.2498	0.0332	0.2944	0.2517	0.0359
C_1	0.0595	0.0527	0.0030	0.0560	0.0498	-	0.0595	0.0527	-	0.0595	0.0527	0.0030
C_{2-3}	0.0339	0.0353	0.0005	0.0316	0.0339	-	0.0337	0.0352	-	0.0339	0.0353	0.0005
C_{4-6}	0.0413	0.0514	6.644E-05	0.0379	0.0506	-	0.0409	0.0513	-	0.0413	0.0514	6.644E-05
C_{7-14}	0.0748	0.1215	2.112E-06	0.0673	0.1240	-	0.0739	0.1218	-	0.0748	0.1215	2.112E-06
C_{15-24}	0.0341	0.0856	3.114E-09	0.0292	0.0908	-	0.0335	0.0862	-	0.0341	0.0856	-
C_{25+}	0.0134	0.0820	3.662E-11	0.0099	0.0869	-	0.0129	0.0828	-	0.0134	0.0820	-
Phase Fraction	0.7079	0.1530	0.1389	0.7547	0.1675	0.0776	0.7140	0.1544	0.1315	0.7079	0.1530	0.1389

Table 2
Comparison of phase compositions obtained with the three different methods for the water/CO_2/NWE-oil mixture at 470 bar and 620 K.

Component	Full Three-Phase Flash			Three-Phase AFWF - 1			Three-Phase AFWF - 5		
	y_i	x_i	w_i	y_i	x_i	w_i	y_i	x_i	w_i
H_2O	0.4683	0.3894	0.9411	0.4817	0.3882	0.9554	0.4683	0.3894	0.9411
CO_2	0.2730	0.2568	0.0522	0.2702	0.2523	0.0445	0.2730	0.2568	0.0522
C_1	0.0551	0.0534	0.0051	0.0546	0.0528	-	0.0551	0.0534	0.0051
C_{2-3}	0.0319	0.0337	0.0011	0.0313	0.0335	-	0.0319	0.0337	0.0011
C_{4-6}	0.0397	0.0464	0.0514	0.0385	0.0464	-	0.0397	0.0464	0.0002
C_{7-14}	0.0748	0.1016	1.928E-05	0.0716	0.1032	-	0.0748	0.1016	1.928E-05
C_{15-24}	0.0372	0.0644	1.053E-07	0.0347	0.0667	-	0.0372	0.0644	-
C_{25+}	0.0196	0.0539	3.123E-09	0.0171	0.0565	-	0.0196	0.0539	-
Phase Fraction	0.7928	0.0870	0.1201	0.7777	0.0688	0.1533	0.7928	0.0870	0.1201

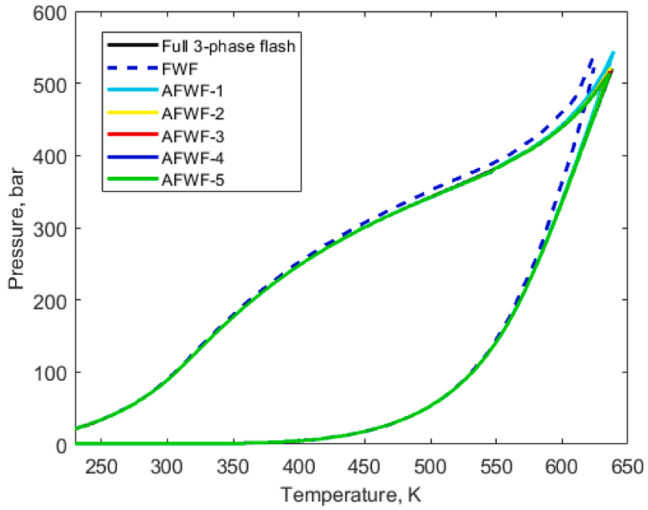

Fig. 2. Three-phase envelopes for the water/CO_2/NWE-oil mixture.

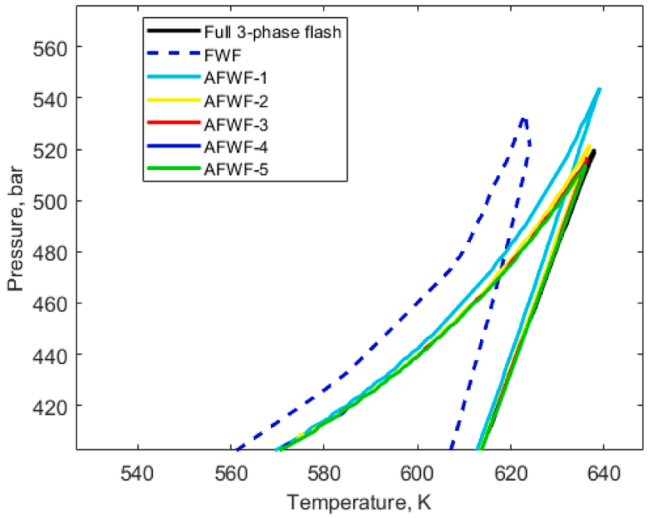

Fig. 3. Detail of the three-phase envelopes for the water/CO_2/NWE-oil mixture at high pressure and temperature.

temperature are relatively high and close to the critical point. This can be seen in Fig. 6, where the spectral radius is calculated for an isobar for water/CO_2/NWE-oil mixture. AFWF with only CO_2 component dissolved in water has the lowest maximum eigenvalue, as compared with full three-phase flash and AFWF with 5 components dissolved in water phase. The relation between the spectral radius of the convergence matrix **S** and the number of iterations can clearly be seen in Fig. 7, which depicts the number of iterations of each method. The higher the spectral radius, the higher is the number of iterations. For the water/CO_2/NWE-oil mixture at 450 bar, even though it is a high pressure, there is not a significant difference in the phase distribution, as presented in Fig. 8. For this particular case, it is clear that using the AFWF with only CO_2 dissolved in the aqueous phase is more advantageous not only because it requires less iterations to converge, but also because it gives a good accuracy.

Let us now look at the Gershgorin bounds of the eigenvalues of the matrix **S**

$$R_{iS} = \sum_{\substack{j=1 \\ i \neq j}}^{nc+m} \left| S_{ij} \right|; i = 1, nc + m \tag{52}$$

where R_{iS} are the Gershgorin radii, which bound the eigenvalues of the matrix [53]. Every eigenvalue of the matrix **S** lies within at least one of the Gershgorin discs, $D(S_{ii}, R_{iS}); i = 1, nc + m$.

In Fig. 9, the Gershgorin bounds are depicted for AFWF with ns=1 and ns=5 and the full flash at 450 bar and 615 K. This figure clearly shows that the length of the intervals containing the eigenvalues of **S** are decreasing when fewer components are dissolved in water. In other words, it is expected to have smaller eigenvalues as ns decreases, with

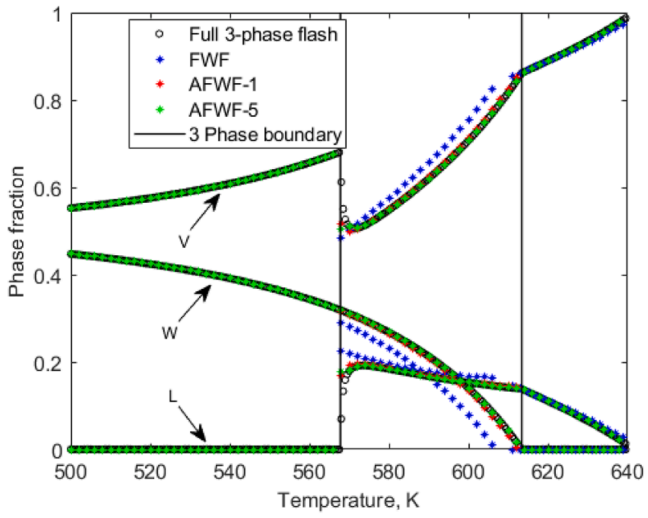

Fig. 4. Phase fractions for full multiphase method, free water flash and with augmented method for partial solubility for the water/CO_2/NWE-oil mixture at 400 bar.

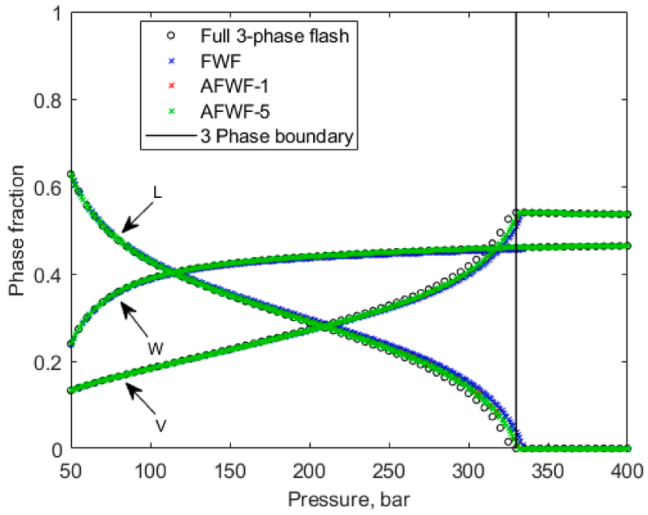

Fig. 5. Phase fractions for full multiphase method, free water flash and with augmented method for partial solubility for the water/CO_2/NWE-oil mixture at 480 K.

Table 3
Maximum eigenvalue at the solution, number of iterations and phase fractions for different ns for the water/CO_2/NWE-oil mixture at 450 bar and 615 K.

Method	Max $\|\lambda_i\|$	Iterations	L	V	W
Full 3-Phase flash-SSI	0.968433	521-SSI	0.139882	0.764563	0.095555
AFWF-SSI-5	0.968433	503-SSI	0.139882	0.764563	0.095555
AFWF-SSI-3	0.968263	495-SSI	0.140363	0.764695	0.094942
AFWF-SSI-1	0.964039	451-SSI	0.152987	0.765798	0.081214

favorable impact on convergence properties.

In Fig. 10, the number of iterations in phase split calculations versus temperature is shown for the AFWF with only CO_2 dissolved in the aqueous phase and full three-phase flash with SSI and SSI-Newton methods for the water/CO_2/NWE-oil mixture at P=80 bar. Convergence is obtained in 6 to 8 iterations using the combined SSI-Newton method in the AFWF and the full three-phase flash. At this moderate pressure, it suffices to consider only the CO_2 dissolution in water; if *ns*

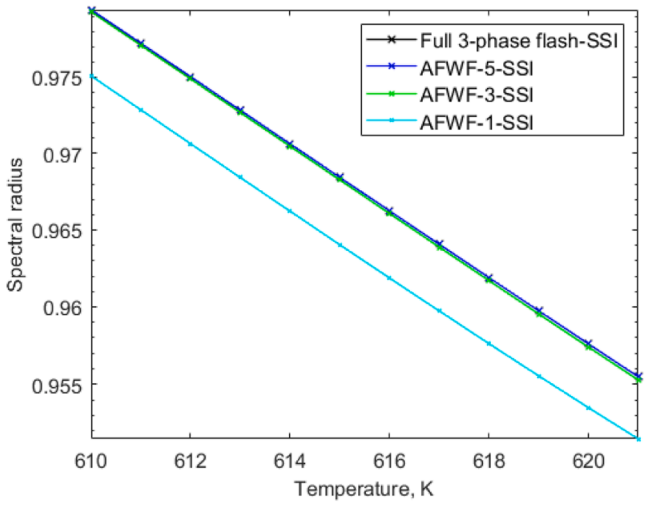

Fig. 6. Maximum eigenvalue of matrix S at the solution for each flash method for the water/CO_2/NWE-oil mixture at 450 bar.

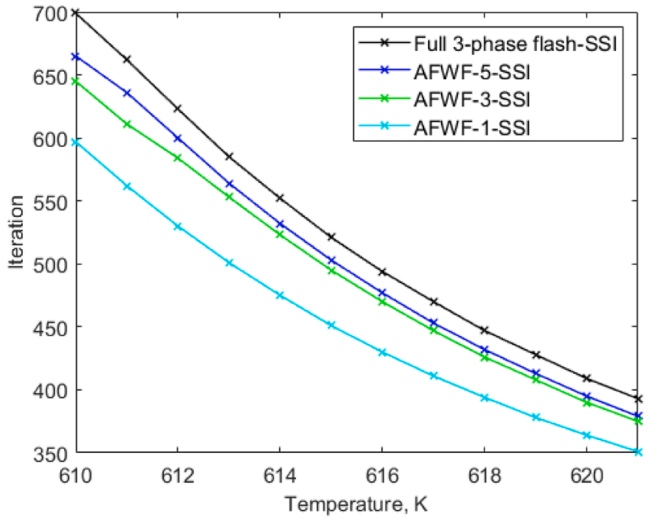

Fig. 7. Number of phase split iterations for the water/CO_2/NWE-oil mixture at 450 bar.

increases, no significant improvements are expected. The Euclidean norm is plotted versus iterations in Fig. 11 at 450 bar and 615 K. As expected, for both SSI and SSI-Newton methods, the AFWF performs slightly better than the full flash. From this example, it is clear that SSI alone is extremely slow, while AFWF requires for convergence only 6 SSI iterations, followed by 5 Newton iterations.

The condition number of the Hessian matrix also gives valuable information when comparing different methods [45]. The condition number of **H** at the solution and phase fractions are listed in Table 4, for full flash and AFWF with five, three, and one component dissolved in water at 450 bar and 615 K. In this example, all considered AFWF converge faster than the full flash, requiring a smaller number of SSI iterations before the switch.

In Fig. 12, the phase distributions are drawn for full three-phase flash and AFWF at 450 bar, showing they are fairly close to each other; even using the AFWF with only CO_2 dissolved in the aqueous phase it is possible to reach basically the same composition as in the conventional flash. In Fig. 13, the number of iterations versus temperature is shown at the same pressure. The number of iterations is clearly decreasing with the number of components soluble in water, the faster being the AFWF with only CO_2 dissolved. The condition number is plotted vs

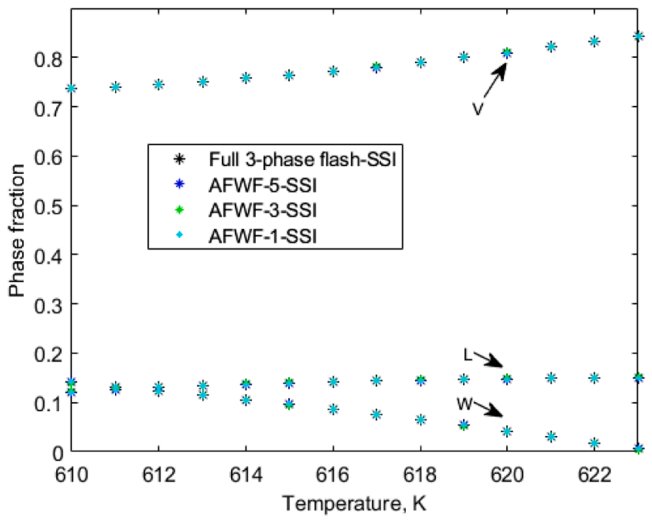

Fig. 8. Phase fractions for each method for the water/CO_2/NWE-oil mixture at 450 bar.

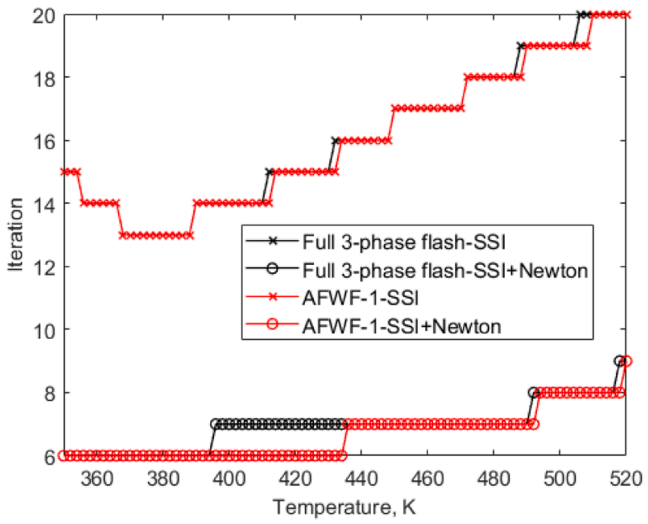

Fig. 10. Number of iterations for the water/CO_2/NWE-oil mixture at 80 bar, considering AFWF with only CO_2 dissolved in the aqueous phase and the conventional full three-phase flash.

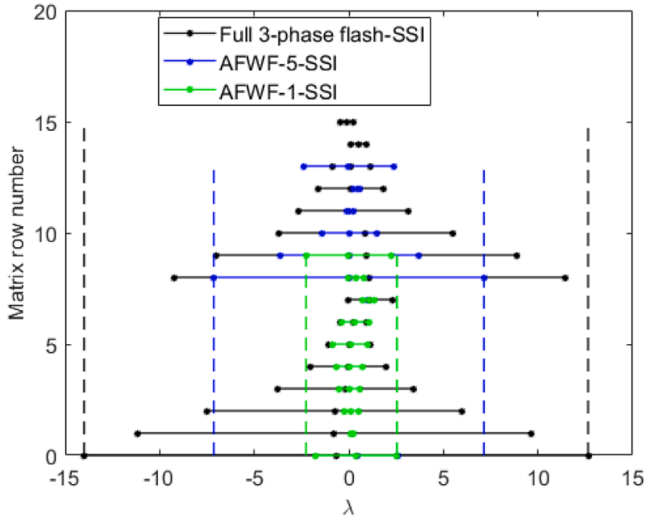

Fig. 9. Gershgorin bounds at the solution for the full flash and augmented free-water flash with one and five components dissolved in water for the water/CO_2/NWE-oil mixture at 450 bar and 615 K.

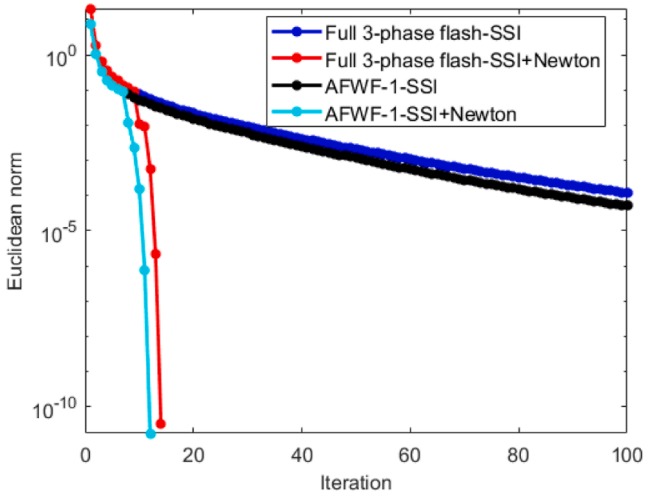

Fig. 11. Euclidean norm as a function of iterations for the full flash and augmented flash for the water/CO_2/NWE-oil mixture at 450 bar and 615 K.

temperature at 450 bar in Fig. 14, and it is clear that the condition number has a direct relation to the number of iterations necessary to reach convergence; the lower the condition number, the lower the number of iterations.

As a general remark, the AFWF systematically showed an advantage in terms of the number of iterations over the full three-phase flash; when the number of components dissolved in water is increased, the number of iterations is also increasing, but it is still lower than for the full flash.

3.2. CO_2/water/ Bob Slaugther Block (BSB)-oil mixture

The Bob Slaugther Block (BSB) oil mixture has a CO_2 concentration higher than 55% and a wide three-phase region. This study uses a ratio of 15:2:3 for water, CO_2, and BSB oil, respectively, as used in Pang and Li [24]. Table B3 lists the component properties and Table B4 presents the non-zero binary BIPs.

3.2.1. Accuracy of FWF and AFWF

Fig. 15 presents the phase envelope in thr *P-T* plane for the water/CO_2/BSB-oil mixture obtained after using the conventional three-phase flash, and matches the results in Ref. [24]. Table 5 presents phase compositions and phase fractions for three different methods, the full flash, FWF and AFWF at 360 bar and 630 K. In the augmented flash, two cases are shown, one that considers only one component dissolved in water, and the other with five components. The higher the number of components used in the mixture for the AFWF, the closer the results to the reference solution. At higher pressure and temperature, 390 bar and 650 K, respectively, phase mole fractions are listed in Table 6. At these conditions, only two phases are predicted by the FWF method and the gap between the results for AFWF with only one component dissolved in aqueous phase and the results for conventional flash are significant, as can be clearly seen when looking at CO_2 and H_2O mole fractions in the aqueous phase.

The phase boundaries of the three-phase region, constructed using the full method, FWF, and AFWF (with several values of *ns*), are drawn in Fig. 16, with a detail in Fig. 17. The FWF reaches a good agreement with the curve obtained from the full method, except for relatively high pressures and temperatures. For temperatures higher than 400 K, the deviation between the phase boundary given by FWF and the one given

Table 4
Condition number, iterations and phase fractions for different ns for the water/CO_2/NWE-oil mixture at 450 bar and 615 K.

Method	Condition number	Iterations	L	V	W
Full 3-Phase flash SSI+Newton	3.76E+11	9-SSI + 5-Newton	0.139882	0.764563	0.095555
AFWF- 5 SSI+Newton	3.51E+07	6-SSI + 5-Newton	0.139882	0.764563	0.095555
AFWF- 3 SSI+Newton	4.12E+05	6-SSI + 5-Newton	0.140363	0.764695	0.094942
AFWF -1 SSI+Newton	6.74E+03	5-SSI + 5-Newton	0.152987	0.765798	0.081214

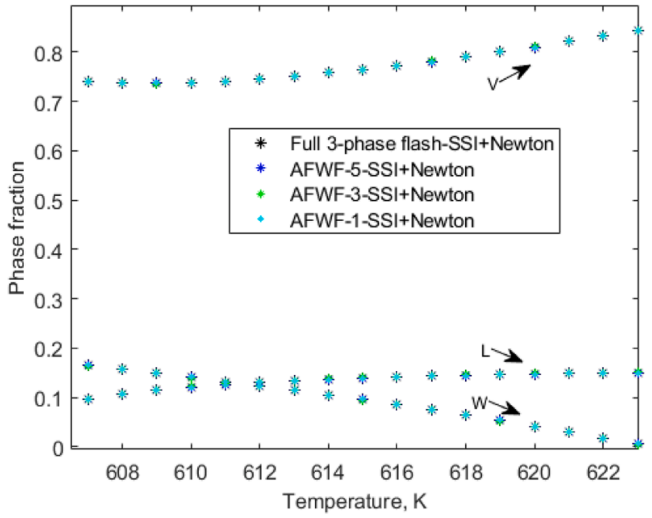

Fig. 12. Phase fractions for each flash method for the water/CO_2/NWE-oil mixture at 450 bar.

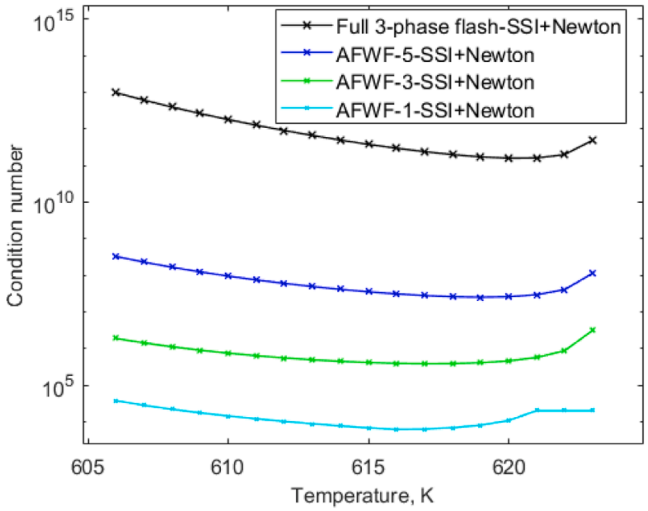

Fig. 14. Condition number of the Hessian matrix at the solution for phase split calculation using SSI and Newton methods for the water/CO_2/NWE-oil mixture at 450 bar.

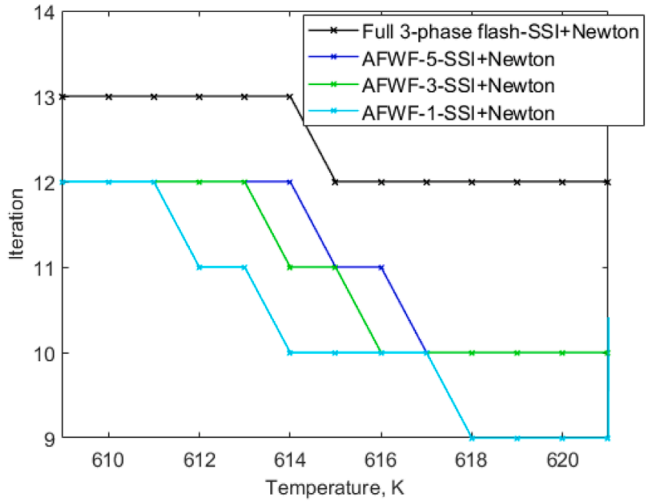

Fig. 13. Number of phase split iterations for the water/CO_2/NWE-oil mixture at 450 bar.

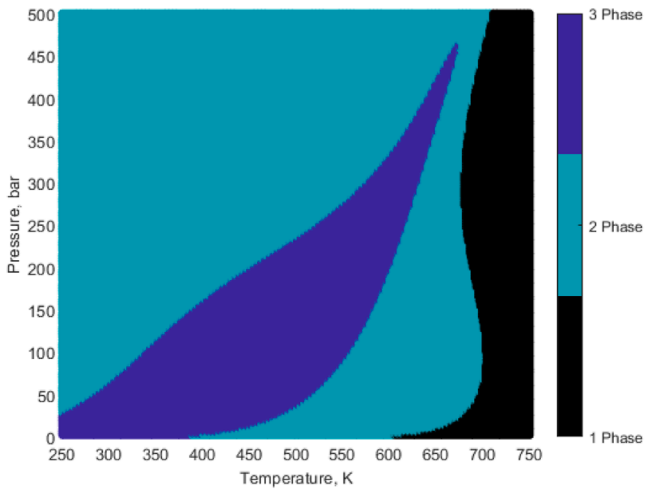

Fig. 15. Phase envelope of the water/CO_2/BSB-oil mixture.

by the conventional flash becomes significant, especially for high pressures. The envelope calculated using the augmented method basically overlaps the one calculated using the conventional flash method for temperatures lower than 600 K. Nevertheless, as seen in Fig. 17, for higher pressure and temperature the augmented method only gets closer to the expected solution when the number of components present in the water phase increases.

The phase distribution calculated with the full three-phase flash, the FWF and the AFWF at T=500 K is shown in Fig. 18. The results are similar to the ones obtained in Ref. [24]. As the pressure increases in the three-phase region, the aqueous phase fraction increases rapidly, while the hydrocarbon liquid phase levels up steadily and vapor fraction decreases. Moreover, the FWF increases its deviation with respect to the full three-phase flash as the pressure increases, as a result of increased solubility of CO_2 and hydrocarbon components in the aqueous phase.

Fig. 19 shows phase distribution for the three flash methods at 220 bar, matching the results from Pang and Li [24]. In this case, phase fractions calculated with the FWF present some deviations at high pressures, while AFWF results are closer to the ones from the full three-phase flash.

3.2.2. *Convergence analysis*

The maximum eigenvalue of the matrix **S**, the number of SSI iterations, and phase fractions at 350 bar and 620 K are presented in Table 7, to compare the full flash and the augmented method considering one,

Table 5
Comparison of phase compositions obtained with the three different methods for the water/CO_2/BSB-oil mixture at 360 bar and 630 K.

Component	Full Three-Phase Flash			Three-Phase FWF			Three-Phase AFWF - 1			Three-Phase AFWF - 5		
	y_i	x_i	w_i	y_i	x_i	w_i	y_i	x_i	w_i	y_i	x_i	w_i
H_2O	0.6087	0.4378	0.9631	0.6934	0.4376	1.0000	0.6231	0.4347	0.9721	0.6087	0.4378	0.9631
CO_2	0.1688	0.1484	0.0321	0.1500	0.1338	-	0.1650	0.1442	0.0278	0.1688	0.1484	0.0321
C_1	0.0219	0.0196	0.0024	0.0183	0.0171	-	0.0227	0.0203	-	0.0219	0.0196	0.0024
C_{2-3}	0.0389	0.0422	0.0017	0.0303	0.0374	-	0.0382	0.0421	-	0.0389	0.0422	0.0017
C_{4-6}	0.0427	0.0554	0.0004	0.0317	0.0513	-	0.0407	0.0546	-	0.0427	0.0554	0.0004
C_{7-15}	0.0782	0.1388	2.233E-05	0.0540	0.1440	-	0.0734	0.1394	-	0.0782	0.1388	2.233E-05
C_{16-27}	0.0316	0.0944	1.30E-07	0.0184	0.1083	-	0.0290	0.0979	-	0.0316	0.0944	-
C_{28+}	0.0088	0.0630	5.04E-09	0.0035	0.0701	-	0.0075	0.0665	-	0.0088	0.0630	-
Phase Fraction	0.4411	0.1080	0.4507	0.5908	0.1224	0.2866	0.4720	0.1068	0.4211	0.4411	0.1080	0.4507

Table 6
Comparison of phase compositions obtained with the three different methods for the water/CO_2/BSB-oil mixture at 390 bar and 650 K.

Component	Full Three-Phase Flash			Three-Phase AFWF - 1			Three-Phase AFWF - 5		
	y_i	x_i	w_i	y_i	x_i	w_i	y_i	x_i	w_i
H_2O	0.7041	0.4900	0.9492	0.7420	0.4903	0.9693	0.7042	0.4899	0.9493
CO_2	0.1333	0.1241	0.0417	0.1231	0.1179	0.0307	0.1333	0.1241	0.0417
C_1	0.0169	0.0164	0.0037	0.0158	0.0162	-	0.0169	0.0164	0.0036
C_{2-3}	0.0294	0.0357	0.0036	0.0263	0.0348	-	0.0294	0.0357	0.0036
C_{4-6}	0.0320	0.0485	0.0016	0.0275	0.0475	-	0.0320	0.0485	0.0015
C_{7-15}	0.0573	0.1308	2.689E-04	0.0463	0.1333	-	0.0573	0.1308	2.668E-04
C_{16-27}	0.0216	0.0936	6.707E-06	0.0157	0.0985	-	0.0216	0.0936	-
C_{28+}	0.0054	0.0608	4.922E-07	0.0033	0.0616	-	0.0054	0.0608	-
Phase Fraction	0.5794	0.1245	0.2960	0.6753	0.1373	0.1874	0.5797	0.1245	0.2958

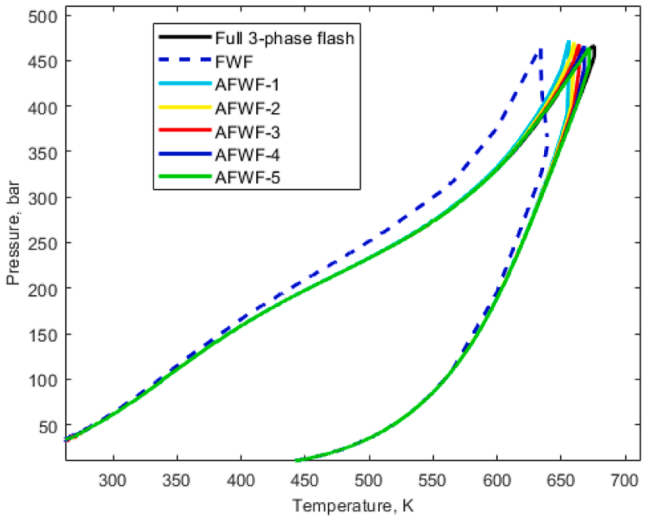

Fig. 16. Three-phase envelopes for the water/CO_2/BSB-oil mixture.

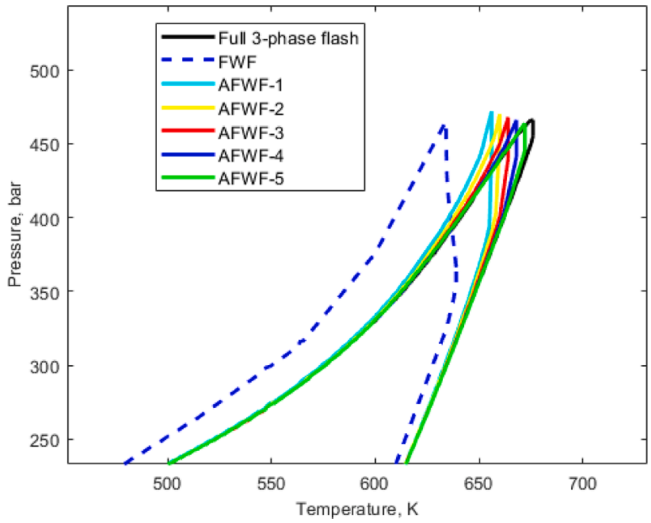

Fig. 17. Detail of the three-phase envelopes for the water/CO_2/BSB-oil mixture.

three, and five components in water rich phase. As expected, the number of iterations increases with the value of the maximum eigenvalue.

Fig. 20 presents the spectral radius of the matrix **S** along the P=350bar isobar. The AFWF method with only CO_2 component dissolved in water has the lowest maximum eigenvalue as compared to the full three-phase flash and the augmented method with five components dissolved in water phase. The relation between the spectral radius of the convergence matrix **S** and the number of iterations for each method is given in Fig. 21; the higher the spectral radius, the higher is the number of iterations. However, we must note that phase fractions are different from the exact solution, as shown in Fig. 22.

The Gershgorin bounds are plotted in 23 for AFWF with ns=1 and ns=5 and the full three-phase flash at 300 bar and 580 K. Again, the length of the intervals containing the eigenvalues of **S** are decreasing when less components are dissolved in water, with favorable impact on convergence properties.

The proposed AFWF method has the advantage of being flexible concerning the number of components dissolved in the aqueous phase, ranging from no component dissolved in aqueous (FWF) to all components present in the mixture dissolved in the aqueous phase (the full flash). Beyond this advantage, the inclusion of a second order method reduces significantly the computational effort of three-phase flash calculations for hydrocarbon/CO_2/water mixtures with respect to the use of SSI alone.

The number of SSI+Newton iterations for FWF, AFWF and full flash calculations is plotted vs temperature at P=300 bar in Fig. 24 and the phase distributions at the same pressure are drawn in Fig. 25. The FWF is more efficient, but the discrepancy in terms of composition is considerable, as seen in Fig. 25, and it confirms that for relatively high

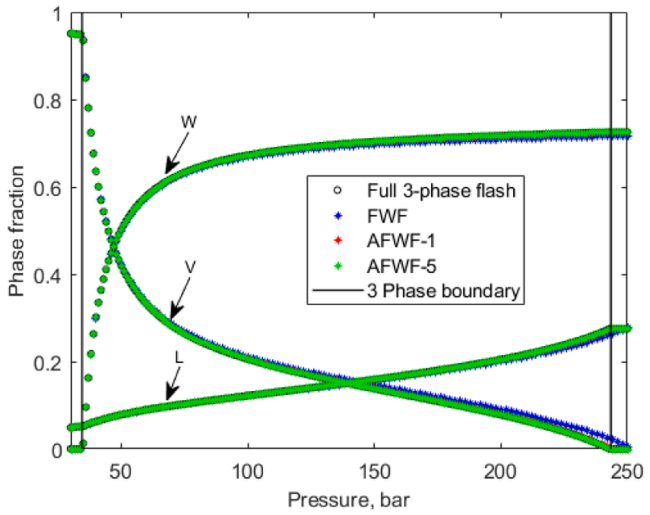

Fig. 18. Comparison of phase distribution for full flash, free-water flash, and augmented free-water flash for the water/CO_2/BSB-oil mixture at 500 K.

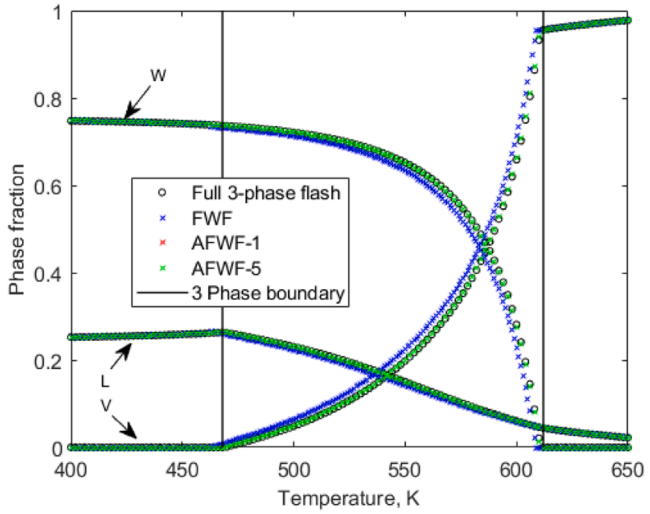

Fig. 19. Comparison of phase distribution for full flash, free-water flash and augmented free-water for the water/CO_2/BSB-oil mixture at 220 bar.

Table 7
Maximum eigenvalue at the solution, iterations and phase fractions for the water/CO_2/BSB-oil mixture at 350 bar and 620 K.

Method	Max $\|\lambda_i\|$	Iterations	L	V	W
3-Phase flash-SSI	0.959018	326-SSI	0.112915	0.374663	0.512422
AFWF-SSI-5	0.959017	306-SSI	0.112915	0.374664	0.512422
AFWF-SSI-3	0.958484	302-SSI	0.112499	0.376765	0.510735
AFWF-SSI-1	0.951465	290-SSI	0.110312	0.395399	0.494290

pressures, using the free water assumption may give significant deviations from the full three-phase flash. The AFWF is slightly faster than the full flash and phase distributions are closer to the exact ones as more components are considered in the aqueous phase.

In Fig. 26, the Euclidean norm variation during iterations is depicted at 300 bar and 610 K for the SSI and SSI+Newton methods. The latter method converges in 8–9 iterations, while using SSI alone requires more than 120 iterations for convergence.

The condition number of the Hessian at the solution, the number of iterations and the phase fractions at 300 bar and 610 K are shown in Table 8 for the full flash and augmented free-water flash with five, three,

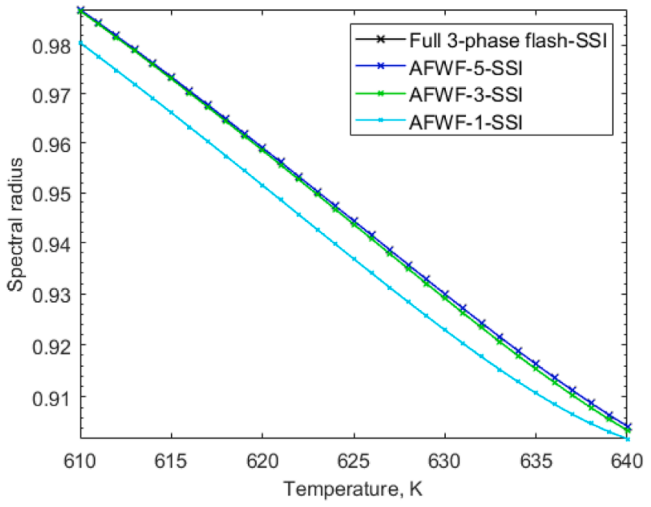

Fig. 20. Maximum eigenvalue at the solution for each method for the water/CO_2/BSB-oil mixture at 350 bar.

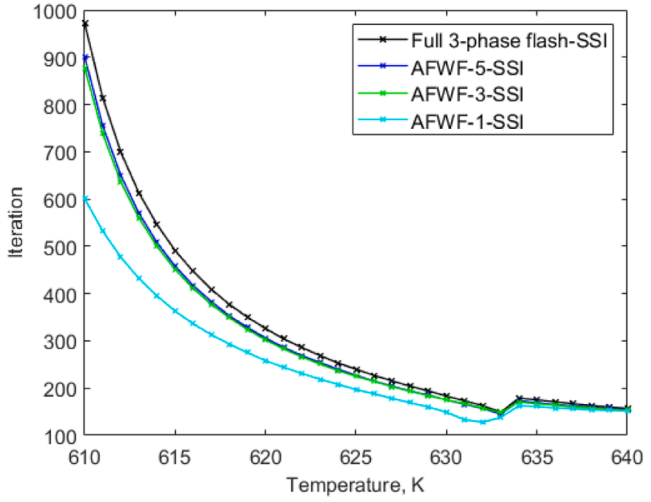

Fig. 21. Number of phase split iterations using SSI for each method for the water/CO_2/BSB-oil mixture at 350 bar.

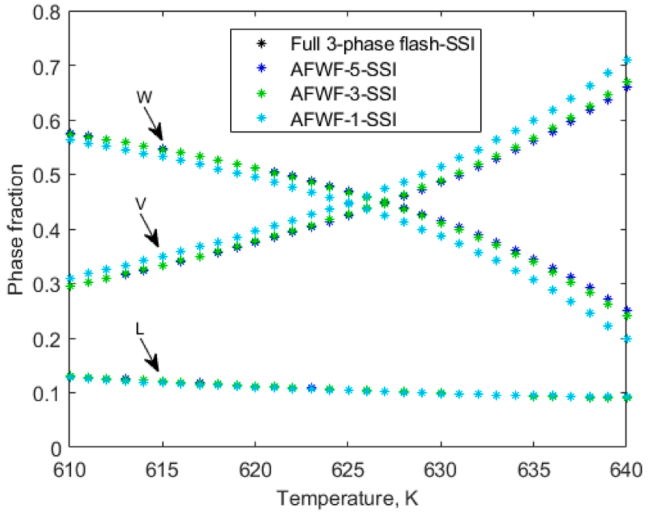

Fig. 22. Phase fractions for each method for the water/CO_2/BSB-oil mixture at 350 bar.

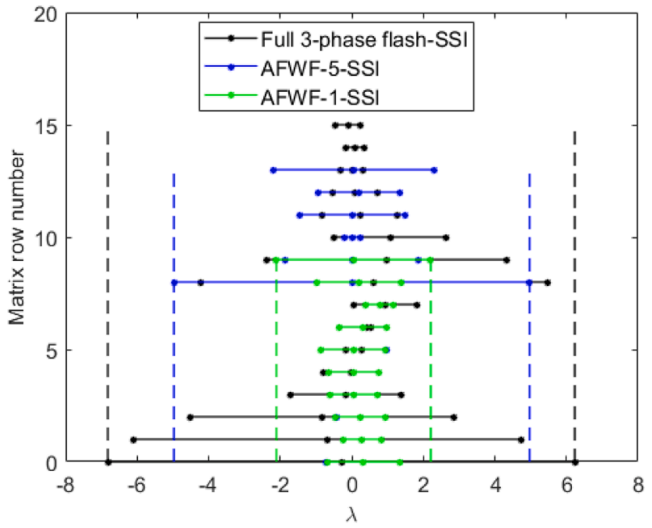

Fig. 23. Gershgorin bounds at the solution for the full flash and augmented free-water flash with one and five components in dissolved in water for the water/CO_2/BSB-oil mixture at 300 bar and 580 K.

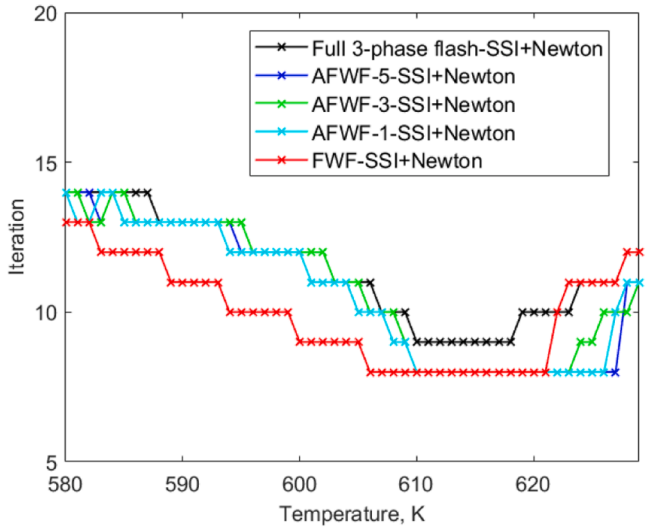

Fig. 24. Comparison of number of iterations for the water/CO_2/BSB-oil mixture at 300 bar.

and one component dissolved in water rich liquid phase. The condition number can vary with several order of magnitude and influences the number of iterations necessary to reach convergence.

The phase fraction distribution at 350 bar is presented In Fig. 27. The results of the AFWF with only CO_2 dissolved in the aqueous phase are different from the ones obtained with the full three-phase flash for the entire temperature range, and these deviations increase with temperature. At the same pressure, the number of iterations and the condition number of the Hessian at the solution are plotted in Figs. 28 and 29, respectively. As the number of dissolved component in the aqueous phase decreases, AFWF is slightly faster and the condition number is decresing.

3.3. Water/gas condensate mixture

A synthetic gas-condensate mixture containing 75% of water [25] is used to test the AFWF for partial solubility of hydrocarbon components in the aqueous phase. Component properties and BIPs from Pang and Li [25] are listed in Table B5.

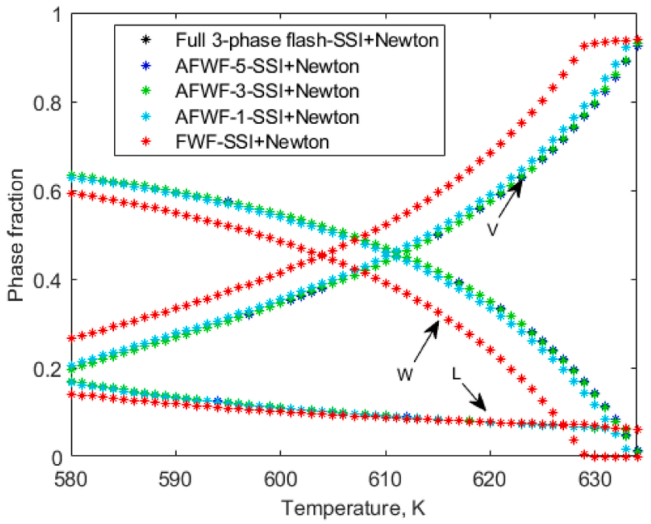

Fig. 25. Phase fraction distribution for the water/CO_2/BSB-oil mixture at 300 bar.

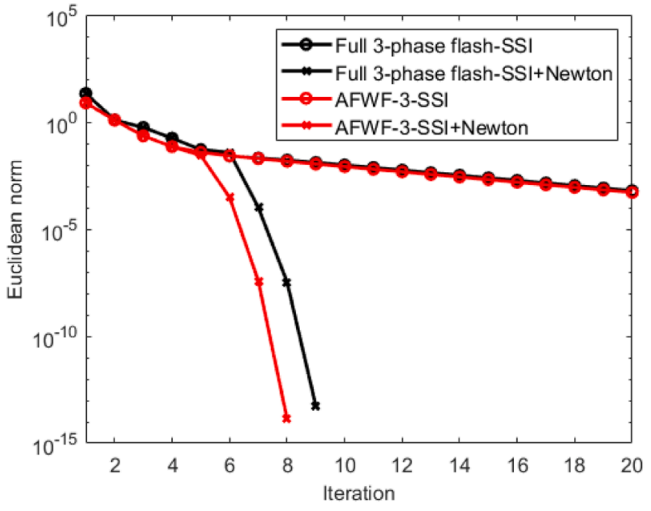

Fig. 26. Comparison of number of iterations for the water/CO_2/BSB-oil mixture at 300 bar and 580 K.

Table 8
Condition number, iterations and phase fractions for different *ns* for the water/CO_2/BSB-oil mixture at 300 bar and 610 K.

Method	Condition number	Iterations	L	V	W
3-Phase flash-Newton	1.64E+11	6-SSI + 3-Newton	0.091507	0.439075	0.469417
AFWF-Newton-5	4.42E+06	5-SSI + 3-Newton	0.091507	0.439075	0.469417
AFWF-Newton-3	1.25E+04	4-SSI +4-Newton	0.091409	0.439854	0.468737
AFWF-Newton-1	2.72E+03	4-SSI + 4-Newton	0.090276	0.450684	0.45904

3.3.1. Accuracy of FWF and AFWF

The phase boundaries of the three-phase region are drawn in Fig. 30 for the conventional three-phase flash, free-water flash, and augmented

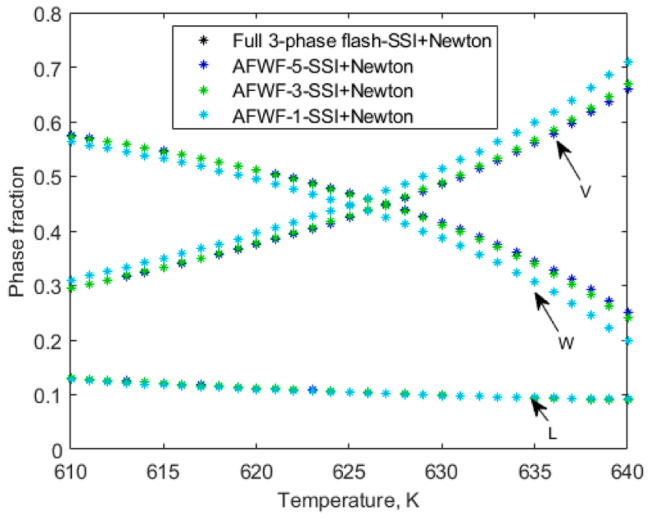

Fig. 27. Phase fractions for each flash method for the water/CO_2/BSB-oil mixture at 350 bar.

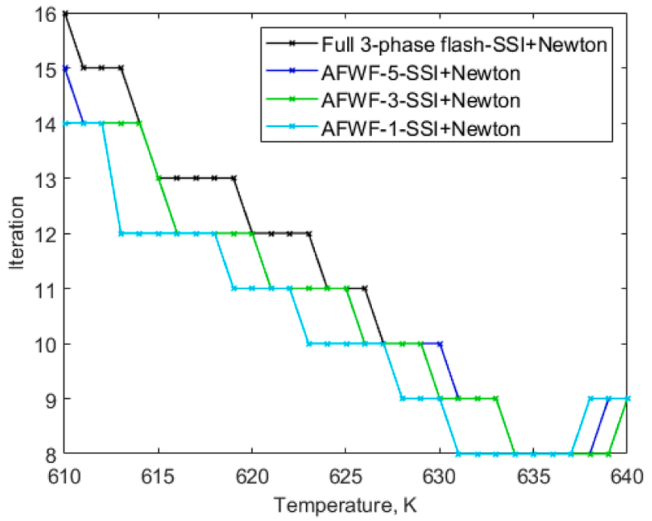

Fig. 28. Number of phase split iterations for the water/CO_2/BSB-oil mixture at 350 bar.

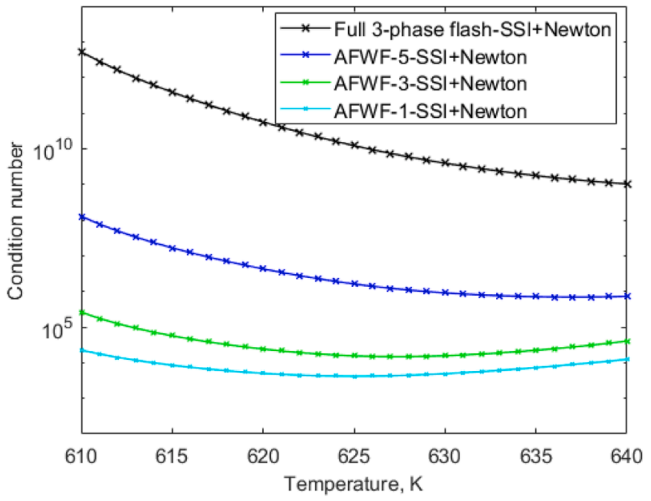

Fig. 29. Condition number of the Hessian matrix at the solution for phase split calculation for the water/CO_2/BSB-oil mixture at 350 bar.

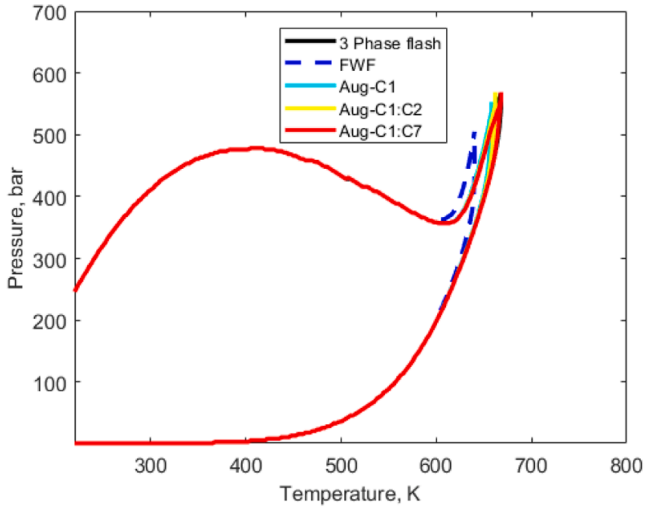

Fig. 30. Phase envelopes for the water/gas condensate mixture. Conventional three-phase flash, FWF, and augmented free water-flash for different solubilities.

free-water flash with one, two, and seven hydrocarbon components dissolved in the aqueous phase. All the curves are very close one to another for temperatures lower than 600 K, but for higher temperatures, the free water flash deviates considerably from the full three-phase flash. For the AFWF, all the curves are closer to the exact solution than the free-water flash. The case with only methane dissolved in water is still far from the full flash for higher temperatures and pressures; however, as the number of components allowed in the water phase increases, the solution gets closer to the one from three-phase flash, as can be seen in Fig. 31.

The mole fractions for each method for the water/gas condensate mixture at 360 bar and 630 K are listed in Table 9. Following the same trend as for the water/CO_2/NWE and water/CO_2/BSB, the augmented free-water flash is very close to the full three-phase flash, while the free-water flash has a higher deviation. Since the amount of C_1 is relatively high, and as this hydrocarbon has a relatively high solubility in water, neglecting the solubility of this component in the aqueous phase is not a good approximation at higher pressures. For an even higher pressure and temperature (430 bar and 645 K), as shown in Table 10, the FWF gives a two-phase response. The AFWF with *ns*=1 have a significant difference for both phase fractions and composition, while the AFWF with seven components is very close to the reference method.

The phase distributions for full three-phase flash and AFWF with one, four, and seven components dissolved in water are presented in Fig. 32. For a pressure of 400 bar at different temperatures, the AFWF-1 deviates considerably from the reference result, while the augmented method with a greater number of components dissolved in the aqueous phase gets closer to the expected solution. For high pressures and temperatures, a larger number of components must be included in the aqueous phase to reduce the deviation from the full three-phase flash solution. A case in which the phase mole fractions calculated with the FWF has relatively small differences with respect to the full three-phase flash as shown in Fig. 33. At a temperature of 470 K, even for higher pressures all methods match well.

3.3.2. *Convergence analysis*

Fig. 34 shows the number of SSI iterations at 400 bar for full three-phase flash and the AFWF. For temperature below 640 K, there is a clear correlation between the number of iterations and the number of components soluble in aqueous phase. However, this is not true anymore

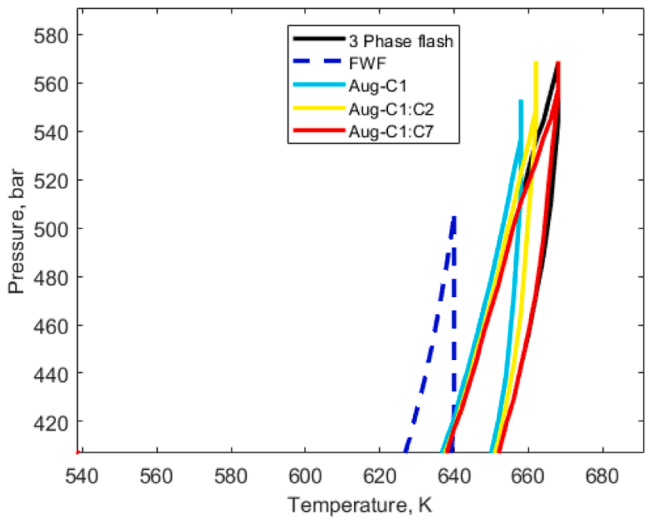

Fig. 31. Detail of the calculated phase envelope for the gas condensate/water mixture.

for temperatures higher than 640 K, since for this case AFWF-1 and AFWF-4 have the highest number of iterations. The number of iterations levels up near the phase boundary for high temperatures where the aqueous phase disappears. Since three-phase phase boundaries of AFWF-1 and AFWF-4 are shifted to the left, the number of iterations is also lagged.

The maximum eigenvalue of the matrix **S**, the number of iterations and phase fractions at 400 bar and 638 K are listed in Table 11 for the AFWF considering seven, four, and one component in aqueous phase and for the full three-phase flash. As expected, the number of iterations increases with the value of the highest eigenvalue; the AFWF-1, which considers only one component dissolved in the aqueous phase, has the lowest number of iterations, but the phase fraction deviates significantly from the full three-phase flash.

The phase distribution at 420 bar is presented in Fig. 35, showing the deviation between results with AFWF-1 and the full flash. The number of SSI+Newton iterations for AFWF and full three-phase flash is depicted in Fig. 36 at the same pressure, showing a decreasing trend when less components are considered in the aqueous phase. For this case, AFWF-4 would be the best option in flash calculation, since it performs better than the full method and AFWF-7, and still give compositions that do not deviate significantly from the full flash.

The condition number of the Hessian at the solution, the number of iterations and phase fractions for the full three-phase flash and the AFWF with one, four, and seven components dissolved in aqueous phase are given in Table 12. It appears that as the condition number increases, the number of iterations also follow the same tendency. The AFWF with only C_1 dissolved in water outperforms the other methods in terms of number of iterations. On the other hand, this particular method shows important deviations of the phase fraction from the full three-phase flash results. Therefore, in this case, the AFWF with four components dissolved in the aqueous phase is preferred, since it gives close phase fraction and has a lower number of iterations as compared to the full three-phase flash method.

4. Conclusions

In this work, a new robust and efficient augmented free-water flash method is proposed for CO_2-water-hydrocarbon mixtures. The new method is general, allowing partial solubility of any selected component in the water-rich phase, depending on the specific compositions and operating conditions. In the general AFWF, the dimension of the problem is reduced; the reduction of the dimensionality is significant if the number of components considered soluble in the aqueous phase is small. The number of components soluble in water is not limited, leading to a controlled accuracy with respect to a full three-phase equilibrium, even

Table 9
Comparison of phase compositions obtained with the three different methods for the water/gas condensate mixture at 360 bar and 630 K.

Component	Full Three-Phase Flash			Free-Water Flash			Three-Phase AFWF - 1			Three-Phase AFWF - 7		
	y_i	x_i	w_i	y_i	x_i	w_i	y_i	x_i	w_i	y_i	x_i	w_i
H_2O	0.6599	0.4484	0.9768	0.7032	0.4505	1.0000	0.6629	0.4486	0.9796	0.6599	0.4484	0.9768
C_1	0.2556	0.2508	0.0218	0.2287	0.2362	-	0.2533	0.2493	0.0204	0.2556	0.2508	0.0218
C_2	0.0172	0.0196	0.0010	0.0152	0.0185	-	0.0174	0.0199	-	0.0172	0.0196	0.0010
C_3	0.0069	0.0089	2.199E-04	0.0060	0.0084	-	0.0069	0.0089	-	0.0069	0.0089	2.199E-04
C_4	0.0070	0.0098	1.182E-04	0.0060	0.0094	-	0.0069	0.0098	-	0.0070	0.0098	1.182E-04
C_5	0.0070	0.0109	7.779E-05	0.0060	0.0106	-	0.0069	0.0109	-	0.0070	0.0109	7.779E-05
C_6	0.0035	0.0062	1.497E-05	0.0029	0.0061	-	0.0034	0.0062	-	0.0035	0.0062	1.497E-05
C_7	0.0070	0.0137	1.427E-05	0.0058	0.0136	-	0.0069	0.0137	-	0.0070	0.0137	1.427E-05
C_{16}	0.0201	0.0951	1.013E-08	0.0154	0.1042	-	0.0198	0.0956	-	0.0201	0.0951	-
C_{29}	0.0160	0.1366	4.080E-09	0.0109	0.1425	-	0.0156	0.1372	-	0.0160	0.1366	-
Phase Fraction	0.6992	0.0099	0.2909	0.7916	0.0273	0.1811	0.7068	0.0108	0.2823	0.6992	0.0099	0.2909

Table 10
Comparison of phase compositions obtained with the three different methods for the water/gas condensate mixture at 430 bar and 645 K.

Component	Full Three-Phase Flash			Three-Phase AFWF - 1			Three-Phase AFWF - 7		
	y_i	x_i	w_i	y_i	x_i	w_i	y_i	x_i	w_i
H_2O	0.6580	0.5014	0.9598	0.6700	0.4999	0.9680	0.6580	0.5014	0.9598
C_1	0.2559	0.2723	0.0373	0.2488	0.2687	0.0320	0.2559	0.2723	0.0373
C_2	0.0173	0.0204	0.0018	0.0173	0.0209	-	0.0173	0.0204	0.0018
C_3	0.0070	0.0090	4.714E-04	0.0069	0.0091	-	0.0070	0.0090	4.713E-04
C_4	0.0071	0.0097	2.928E-04	0.0069	0.0098	-	0.0071	0.0097	2.927E-04
C_5	0.0071	0.0106	2.112E-04	0.0068	0.0106	-	0.0071	0.0106	2.112E-04
C_6	0.0036	0.0058	5.049E-05	0.0034	0.0058	-	0.0036	0.0058	5.047E-05
C_7	0.0071	0.0126	5.681E-05	0.0068	0.0126	-	0.0071	0.0126	5.679E-05
C_{16}	0.0205	0.0728	2.612E-07	0.0186	0.0750	-	0.0205	0.0728	-
C_{29}	0.0164	0.0854	1.179E-07	0.0145	0.0874	-	0.0164	0.0854	-
Phase Fraction	0.6679	0.0179	0.3142	0.6849	0.0297	0.2854	0.6679	0.0179	0.3142

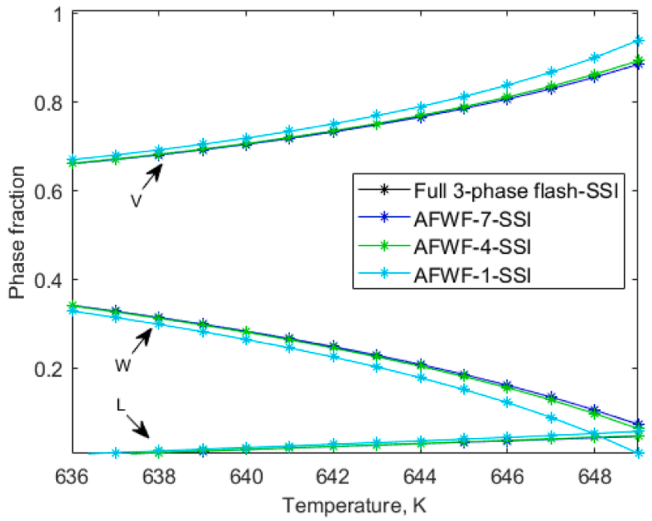

Fig. 32. Phase fractions for each flash method for the water/gas condensate mixture at 400 bar.

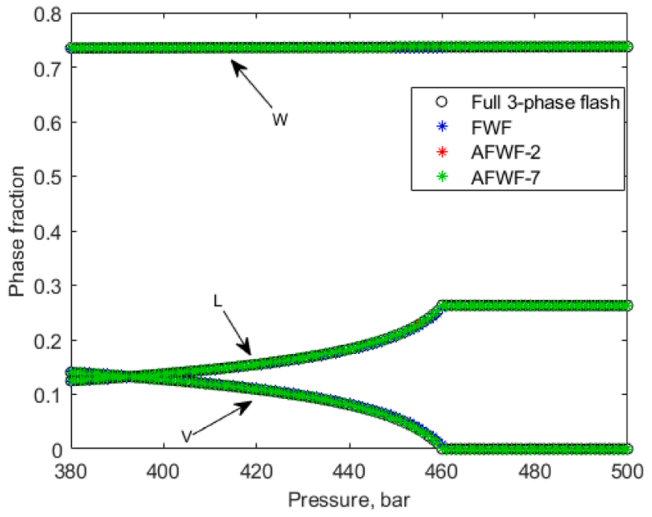

Fig. 33. Phase fractions for each flash method for the water/gas condensate mixture at 470 K.

at high pressures and/or large amounts of CO_2.

All previously published FWF and AFWF methods used the first-order SSI method, which may be very slow. Second-order methods are presented in detail for the first time in this work for solving the AFWF problem. Newton iterations with a modified Cholesky factorization and line search are used in a highly robust combined SSI-Newton sequence.

The new AFWF method is tested for several hydrocarbon-water-CO_2 mixtures and proved to be robust (with no particular convergence issues observed) and efficient, systematically outperforming the conventional full three-phase approach. We have shown for all test examples that the maximum eigenvalue of the convergence S-matrix (which controls the convergence rate of the SSI method) and the condition number of the Hessian matrix (which affects the convergence behavior of the Newton method) are smaller for the AFWF than for the full three-phase flash. This explains why the number of iterations required by the AFWF in both first-and second-order methods is systematically smaller than in the full three-phase flash.

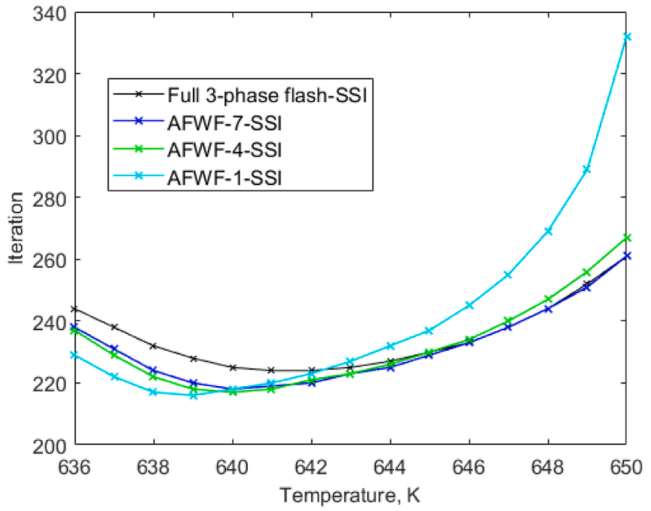

Fig. 34. Number of iterations for each method for the water/gas condensate mixture at 400 bar in the three phase region.

Table 11
Maximum eigenvalue at the solution, iterations and phase fractions for the water/gas condensate fluid mixture at 400 bar and 638 K.

Method	Max $\|\lambda_i\|$	Iterations	L	V	W
3-Phase flash-SSI	0.837333	374-SSI	0.007955	0.679213	0.312832
AFWF-SSI-7	0.837332	224-SSI	0.007955	0.679214	0.312831
AFWF-SSI-4	0.837197	222-SSI	0.008223	0.680611	0.311165
AFWF-SSI-1	0.834787	217-SSI	0.012101	0.690545	0.297354

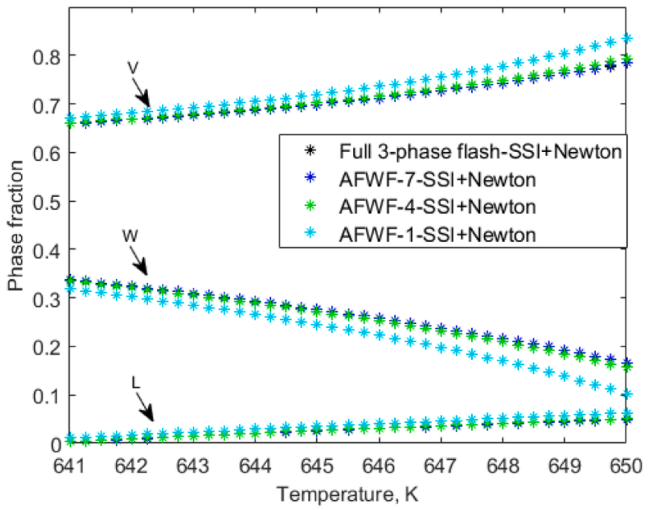

Fig. 35. Phase fractions for different ns for the water/gas condensate mixture at 420 bar.

In our test examples, up to 5% of CO_2 can be dissolved in the aqueous phase. Moreover, we show that at high pressures, solubility of additional components in water must be allowed to reduce deviations with respect to full three-phase flash results in terms of phase boundaries, phase distributions, and mole fractions; the user can choose the desired level of approximation. The AFWF methodology was designed for implementation in compositional reservoir simulators, with applications ranging from CO_2 storage and geothermal projects to a variety of enhanced oil recovery processes.

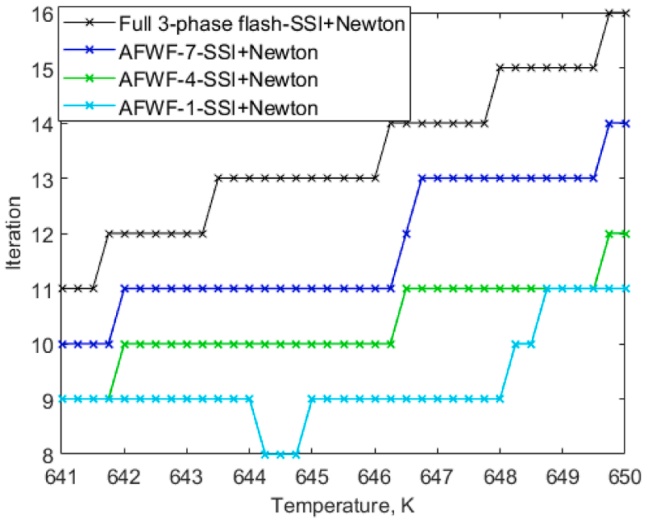

Fig. 36. Number of iterations for different ns for the water/gas condensate mixture at 420 bar in the three phase region.

Table 12
Condition number, iterations and phase fractions for different ns for the water/gas condensate fluid mixture at 420 bar and 650 K.

Method	Condition number	Iterations	L	V	W
3-Phase flash-Newton	1.31E+08	16	0.049503	0.783834	0.166663
AFWF-Hybrid-7	1.92E+06	14	0.049511	0.783896	0.166593
AFWF-Hybrid-4	5.24E+05	12	0.051394	0.792231	0.156375
AFWF- Hybrid-1	1.13E+05	11	0.063343	0.834569	0.102088

CRediT authorship contribution statement

Juan Heringer: Writing – original draft, Validation, Software, Methodology, Formal analysis, Conceptualization. **Michiel Wapperom:** Software, Methodology, Conceptualization. **Catinca Secuianu:** Writing – review & editing, Validation, Methodology, Conceptualization. **Denis Voskov:** Writing – review & editing, Validation, Supervision, Methodology, Funding acquisition, Conceptualization. **Dan Vladimir Nichita:** Writing – review & editing, Writing – original draft, Validation, Supervision, Methodology, Funding acquisition, Formal analysis, Conceptualization.

Declaration of competing interest

The authors declare the following financial interests/personal relationships which may be considered as potential competing interests: Juan Heringer, Michiel Wapperom reports financial support was provided by Total Energies. If there are other authors, they declare that they have no known competing financial interests or personal relationships that could have appeared to influence the work reported in this paper.

Acknowledgements

JH and MW thank Total Energy for financial support. CS and DVN thank the ISIFoR Carnot Institute for a mobility grant.

Appendix A. Derivation of the Q-function from the Gibbs free energy

In the expression of the dimensionless Gibbs free energy

$$G = \sum_{i=1}^{nc} n_{iV} \ln f_{iV} + \sum_{i=1}^{nc} n_{iL} \ln f_{iL} + \sum_{i=1}^{m} n_{iW} \ln f_{iW} \tag{B1}$$

we add and subtract

$$\sum_{i=1}^{nc} z_i \ln z_i = \sum_{i=1}^{nc} n_{iV} \ln z_i + \sum_{i=1}^{nc} n_{iL} \ln z_i + \sum_{i=1}^{m} n_{iW} \ln z_i \tag{B2}$$

we obtain

$$G = \sum_{i=1}^{nc} z_i \ln z_i + \ln P + \sum_{i=1}^{nc} n_{iV} \ln\left(\frac{y_i \varphi_{iV}}{z_i}\right) + \sum_{i=1}^{nc} n_{iL} \ln\left(\frac{x_i \varphi_{iL}}{z_i}\right) + \sum_{i=1}^{m} n_{iW} \ln\left(\frac{w_i \varphi_{iW}}{z_i}\right) \tag{B3}$$

Using the mole fractions and equilibrium constants expressions (Eqs. 4) we get

$$\ln\left(\frac{y_i\varphi_{iV}}{z_i}\right)=\ln\left(\frac{\cancel{z_i}K_{iV}}{E_i}\frac{\varphi_{iV}}{\cancel{z_i}}\right)=\ln\left(\frac{\varphi_{iL}}{\cancel{\varphi_{iV}}}\frac{\cancel{\varphi_{iV}}}{E_i}\right)=\ln\left(\frac{\varphi_{iL}}{E_i}\right);i=1,m \tag{B4a}$$

$$\ln\left(\frac{x_i\varphi_{iL}}{z_i}\right)=\ln\left(\frac{\cancel{z_i}}{E_i}\frac{\varphi_{iL}}{\cancel{z_i}}\right)==\ln\left(\frac{\varphi_{iL}}{E_i}\right);i=1,m \tag{B4b}$$

$$\ln\left(\frac{w_i\varphi_{iW}}{z_i}\right)=\ln\left(\frac{\cancel{z_i}K_{iW}}{E_i}\frac{\varphi_{iW}}{\cancel{z_i}}\right)=\ln\left(\frac{\varphi_{iL}}{\cancel{\varphi_{iW}}}\frac{\cancel{\varphi_{iW}}}{E_i}\right)=\ln\left(\frac{\varphi_{iL}}{E_i}\right);i=1,m \tag{B4c}$$

Similarly,

$$\ln\left(\frac{y_i\varphi_{iV}}{z_i}\right)=\ln\left(\frac{\cancel{z_i}K_{iV}}{\overline{E}_i}\frac{\varphi_{iV}}{\cancel{z_i}}\right)=\ln\left(\frac{\varphi_{iL}}{\cancel{\varphi_{iV}}}\frac{\cancel{\varphi_{iV}}}{\overline{E}_i}\right)=\ln\left(\frac{\varphi_{iL}}{\overline{E}_i}\right);i=m+1,nc \tag{B4d}$$

$$\ln\left(\frac{x_i\varphi_{iL}}{z_i}\right)=\ln\left(\frac{\cancel{z_i}}{\overline{E}_i}\frac{\varphi_{iL}}{\cancel{z_i}}\right)==\ln\left(\frac{\varphi_{iL}}{\overline{E}_i}\right);i=m+1,nc \tag{B4e}$$

Introducing Eqs. (B4) in Eq. (B3) and taking into account Eq. (1) gives

$$G=\sum_{i=1}^{nc}z_i\ln z_i+\ln P+\sum_{i=1}^{nc}z_i\ln\varphi_{iL}-\sum_{i=1}^{m}z_i\ln E_i-\sum_{i=m+1}^{nc}z_i\ln\overline{E}_i \tag{B5}$$

If the fugacity coefficients (thus the equilibrium constants) are not dependent on compositions, that is, the ideal case, G can be written as

$$G=C-Q(V,W) \tag{B6}$$

where

$$Q(V,W)=-\sum_{i=1}^{m}z_i\ln E_i-\sum_{i=m+1}^{nc}z_i\ln\overline{E}_i \tag{B7}$$

is exactly the function from Eq. (30).

If we introduce

$$E_i=S_i\varphi_{iL} \tag{B8a}$$

$$\overline{E}_i=\overline{S}_i\varphi_{iL} \tag{B8b}$$

where

$$S_i=\frac{V}{\varphi_{iV}}+\frac{L}{\varphi_{iL}}+\frac{W}{\varphi_{iW}};i=1,m \tag{B9a}$$

$$\overline{S}_i=\frac{V}{\varphi_{iV}}+\frac{L}{\varphi_{iL}};i=m+1,nc \tag{B9b}$$

in Eq. (B5), Michelsen's Q-function [43] is obtained, as in Yan and Stenby [42].

Appendix B. Composition, component properties and non-zero BIPs

Table B1, Table B2, Table B3, Table B4, Table B5

Table B1
Component properties of water/CO_2/NEW oil mixture.

Component	T_c (K)	P_c (bar)	ω	*Mol*%
H_2O	647.30	220.48	0.344	50.0000
CO_2	304.20	73.76	0.225	25.1925
C_1	190.60	46.00	0.008	5.0625
$C_{2–3}$	343.64	45.05	0.130	2.9500
$C_{4–6}$	466.41	33.50	0.244	3.7100
$C_{7–14}$	603.07	24.24	0.600	7.1575
$C_{15–24}$	733.79	18.03	0.903	3.7250
C_{25+}	923.20	17.26	1.229	2.2025

Table B2
BIPs for water/CO_2/NEW oil mixture.

Component	k_{H2O}	k_{CO2}
H_2O	-	0.1896
CO_2	0.1896	-
C_1	0.4850	0.1200
$C_{2–3}$	0.5000	0.1200
$C_{4–6}$	0.5000	0.1200
$C_{7–14}$	0.5000	0.0900
$C_{15–24}$	0.5000	0.0900
C_{25+}	0.5000	0.0900

Table B3
Component properties of BSB oil mixture.

Component	T_c (K)	P_c (bar)	ω	*Mol*%
H_2O	647.30	220.48	0.344	75.0000
CO_2	304.20	73.76	0.225	10.5055
C_1	160.00	46.00	0.008	1.2915
$C_{2–3}$	344.22	45.00	0.131	2.2545
$C_{4–6}$	463.22	34.00	0.240	2.5065
$C_{7–15}$	605.78	21.75	0.618	4.9560
$C_{16–27}$	751.00	16.54	0.957	2.4165
C_{28+}	942.50	16.42	1.268	1.0695

Table B4
BIPs for water/CO_2/BSB oil mixture.

Component	k_{H2O}	k_{CO2}
H_2O	-	0.1896
CO_2	0.1896	-
C_1	0.4850	0.0550
$C_{2–3}$	0.5000	0.0550
$C_{4–6}$	0.5000	0.0550
$C_{7–15}$	0.5000	0.1050
$C_{16–27}$	0.5000	0.1050
C28+	0.5000	0.1050

Table B5
Component properties and BIPs of water/reservoir mixture.

Component	T_c (K)	P_c (bar)	ω	*Mol*%	k_{H2O}
H_2O	647.30	220.48	0.344	75.00	-
C_1	190.58	46.04	0.011	18.75	0.485
C_2	305.42	48.80	0.099	1.25	0.500
C_3	369.82	42.49	0.152	0.50	0.500
C_4	408.14	36.48	0.177	0.50	0.500

(*continued on next page*)

Table B5 (*continued*)

Component	T_c (K)	P_c (bar)	ω	*Mol*%	k_{H2O}
C_5	464.78	35.29	0.233	0.50	0.500
C_6	507.43	30.12	0.305	0.25	0.500
C_7	540.26	27.36	0.351	0.50	0.500
C_{16}	717.00	14.19	0.742	1.50	0.500
C_{29}	816.55	14.51	1.129	1.25	0.500

Data availability

No data was used for the research described in the article.

References

[1] N. Sabet, H.R.E. Gahrooei, A new robust stability algorithm for three phase flash calculations in presence of water, J. Nat. Gas Sci. Eng. 35 (2016) 382–391. Part A.

[2] E. Mortezazadeh, M.R. Rasaei, A robust procedure for three-phase equilibrium calculations of water-hydrocarbon systems using cubic equations of state, Fluid Phase Equilib 450 (2017) 160–174.

[3] M. Nazari, M.B. Asadi, S. Zendehboudi, A new efficient algorithm to determine three-phase equilibrium conditions in the presence of aqueous phase: phase stability and computational cost, Fluid Phase Equilib 486 (2019) 139–158.

[4] M Connolly, H Pan, H Tchelepi, Three-phase equilibrium computations for hydrocarbon-water mixtures using a reduced variables method, Ind. Eng. Chem. Res. 58 (2019) 14954–14974.

[5] M. Imai, H. Pan, M. Connolly, H Tchelepi, M. Kurihara, Reduced variables method for four-phase equilibrium calculations of hydrocarbon-water-CO2 mixtures at a low temperature, Fluid Phase Equilib 497 (2019) 151–163.

[6] R. Li, H.A. Li, Improved three-phase equilibrium calculation algorithm for water/hydrocarbon mixtures, Fuel 244 (2019) 517–527.

[7] M. Petitfrere, D.V. Nichita, D. Voskov, R. Zaydullin, I. Bogdanov, Full-EoS based thermal multiphase compositional simulation of CO2 and steam injection processes, J. Petrol. Sci. Eng. 192 (2020) 107241.

[8] X. Ma, S. Wu, G. Huang, T. Fan, Three-phase equilibrium calculations of water/hydrocarbon/nonhydrocarbon systems based on the equation of State (EOS) in thermal processes, ACS Omega 6 (2021) 34406–34415.

[9] R. Sun, H. Pan, H. Tchelepi, New algorithm of three-phase equilibrium calculations for CO2-hydrocarbon-water systems, Geoenergy Sci. Eng. 244 (2025) 213426.

[10] D. Zhu, R. Okuno, Robust isenthalpic flash for multiphase water/hydrocarbon mixtures, SPE J 20 (2015) 1350–1365.

[11] D. Huang, D. Yang, A robust multiphase isenthalpic flash model for water/solvent/hydrocarbon systems at high pressures and elevated temperatures, Fluid Phase Equilib 489 (2019) 48–66.

[12] D. Huang, R. Li, D.T. Yang, Multiphase boundaries and physical properties of solvents/heavy oil systems under reservoir conditions by use of isenthalpic flash algorithms, Fuel 298 (2021) 120508.

[13] Y. Tang, S. Saha, An efficient method to calculate three-phase free-water flash for water-hydrocarbon systems, Ind. Eng. Chem. Res. 42 (2003) 189–197.

[14] A. Iranshahr, D.V. Voskov, H.A. Tchelepi, Phase equilibrium computations are No longer the bottleneck in thermal compositional EoS based simulation, SPE 119166, 2009, in: SPE Reservoir Simulation Symposium, The Woodlands, TX, 2009, https://doi.org/10.2118/119166-MS, 2-4 February.

[15] A. Lapene, D.V. Nichita, G. Debenest, M. Quintard, Three-phase free-water flash calculations using a new modified Rachford–Rice equation, Fluid Phase Equilib 297 (2010) 121–128.

[16] R. Li, H.A. Li, New two-phase and three-phase Rachford-Rice algorithms based on free-water assumption, Can. J. Chem. Eng. 96 (2018) 390–403.

[17] S. Li, L. Xu, H. Li, Four-phase flash calculation algorithm based on the free-water assumption, Ind. Eng. Chem. Res. 61 (2022) 3742–3753.

[18] Z. Chen, R. Li, H. Li, An improved vapor-liquid-asphaltene three-phase equilibrium computation algorithm, Fluid Phase Equilib 537 (2021) 113004.

[19] Z. Chen, R. Li, H. Li, A new vapor-liquid-asphaltene three-phase equilibrium computation algorithm based on the free-asphaltene assumption, Fluid Phase Equilib 556 (2022) 113392.

[20] V. Koulocheris, A. Plakia, V. Louli, E. Panteli, E. Voutsas, Calculating the chemical and phase equilibria of mercury in natural gas, Fluid Phase Equilib 544–545 (2021) 113089.

[21] M.A. Cremon, N. Castelletto, J.A. White, Multi-stage preconditioners for thermal–compositional–reactive flow in porous media, J. Comput. Physics 418 (2020) 109607.

[22] M.A. Cremon, M.G. Gerritsen, Multi-level delumping strategy for thermal enhanced oil recovery simulations at low pressure, Fluid Phase Equilib 528 (2021) 112850.

[23] M.A. Cremon, M.G. Gerritsen, Compositional effects in thermal, compositional and reactive simulation, Computational Geosciences 26 (2022) 727–738.

[24] W. Pang, H.A. Li, An augmented free-water three-phase Rachford-Rice algorithm for CO2/hydrocarbons/water mixtures, Fluid Phase Equilib 450 (2017) 86–98.

[25] W. Pang, H.A. Li, Application of augmented free-water Rachford-Rice algorithm to water/hydrocarbons mixtures considering the dissolution of methane in the aqueous phase, Fluid Phase Equilib 460 (2018) 75–84.

[26] Y.K. Li, L.X. Nghiem, Phase equilibria of oil, gas and water/brine mixtures from a cubic equation of state and Henry's law, Can. J. Chem. Eng. 64 (1986) 486–496.

[27] R.M. Enick, S.M. Klara, Effects of CO2 solubility in Brine on the compositional simulation of CO2 floods, SPE Res. Eng. 7 (1992) 253–258.

[28] W. Yan, M.L. Michelsen, E.H. Stenby, R.A. Berenblyum, A.A. Shapiro, Three-phase compositional streamline simulation and its application to WAG, in: SPE/DOE Symposium on Improved Oil Recovery, Tulsa, Oklahoma, 2004, https://doi.org/10.2118/89440-MS. April 17-21.

[29] W. Yan, E.H. Stenby, The influence of CO2 solubility in Brine on CO2 flooding simulation, in: SPE Annual Technical Conference and Exhibition, New Orleans, Louisiana, 2009, https://doi.org/10.2118/124628-MS. October 4-7.

[30] W. Yan, E.H. Stenby, The influence of CO2 solubility in brine on simulation of CO2 injection into water flooded reservoir and CO2 WAG, in: SPE EUROPEC/EAGE Annual Conference and Exhibition, Barcelona, Spain, 2010, https://doi.org/10.2118/131094-MS. June 14-17.

[31] W. Yan, R. Berenblyum, A.A. Shapiro, M.L. Michelsen, E.H. Stenby. Compositional Streamline Simulation Progress Report No. 3. Technical report, Technical University of Denmark, November 2002. Private communication, Wei Yan, June 2024.

[32] D.V. Nichita, Fast and robust three-phase free-water flash calculations, in: AIChE Annual Meeting, Boston (Nov. 7-11) and Virtual (Nov. 15-19), 2021.

[33] P.E. Gill, W. Murray, Newton type methods for unconstrained and linearly constrained optimization, Math. Program. 7 (1974) 311–350.

[34] R.B. Schnabel, E. Eskow, A new modified cholesky factorization, SIAM J. Sci. Stat. Comput. 11 (1990) 1136–1158.

[35] D.V. Nichita, M. Petitfrere, Phase equilibrium calculations with quasi-Newton methods, Fluid Phase Equilib 406 (2015) 194–208.

[36] M. Petitfrère, D.V. Nichita, Robust and efficient Trust-region based stability analysis and multiphase flash calculations, Fluid Phase Equilib 362 (2014) 51–68.

[37] M. Petitfrere, D.V. Nichita, Multiphase equilibrium calculations using a reduction method, Fluid Phase Equilib 401 (2015) 110–126.

[38] M.L. Michelsen, The isothermal problem. Part II. Phase split calculation, Fluid Phase Equilib 9 (1982) 21–40.

[39] C.H. Whitson, M.L. Michelsen, The negative flash, Fluid Phase Equilib 53 (1990) 51–72.

[40] D.V. Nichita, D. Broseta, F. Montel, Calculation of convergence pressure/temperature and stability test limit loci of mixtures with cubic equations of state, Fluid Phase Equilib 261 (2007) 176–184.

[41] C.F. Leibovici, D.V. Nichita, A new look at multiphase Rachford–Rice equations for negative flashes, Fluid Phase Equilib 267 (2008) 127–132.

[42] R.W. Yan, E.H. Stenby, On multiphase negative flash for ideal solutions, Fluid Phase Equilib 322–323 (2012) 41–47.

[43] M.L. Michelsen, Calculation of multiphase equilibrium, Comput. Chem. Eng. 18 (1994) 545–550.

[44] R. Okuno, R.T. Johns, K. Sepehrnoori, A new algorithm for Rachford-Rice for multiphase compositional simulation, SPE J 15 (2010) 313–325.

[45] M. Petitfrere, D.V. Nichita, A comparison of conventional and reduction approaches for phase equilibrium calculations, Fluid Phase Equilib 386 (2015) 30–46.

[46] M. Muskat, J.M. McDowell, An Electrical Computer For Solving Phase Equilibrium Problems, SPE 949291-G, 1949.

[47] D.V. Nichita, C.F. Leibovici, A rapid and robust method for solving the Rachford–Rice equation using convex transformations, Fluid Phase Equilibria 353 (2013) 38–49.

[48] D.V. Nichita, C.F. Leibovici, Improved solution windows for the resolution of the Rachford-Rice equation, Fluid Phase Equilibria 452 (2017) 69–73.

[49] G. Wilson, in: A modified Redlich-Kwong equation of state, application to general physical data calculations. Paper no. 15C presented at the AIChE 65th National Meeting, Cleveland, Ohio, 1969. May 4-7.

[50] M.L. Michelsen, The isothermal problem. Part I. Stability, Fluid Phase Equilib. 9 (1982) 1–19.

[51] D.Y. Peng, D.B. Robinson, A new two-constant equation of State, Ind. Eng. Chem. Fundam. 15 (1976) 59–64.

[52] D.Y. Peng, D.B. Robinson, Two and three phase equilibrium calculations for systems containing water, Can. J. Chem.Eng. 54 (1976) 595–599.

[53] G.H. Golub, J.H. Welsch, Calculation of Gauss quadrature rules, Math. Comp. 2 (1969) 221–230.